

Time evolution of 1D gapless models from a domain-wall initial state: SLE continued?

Pasquale Calabrese¹, Christian Hagendorf², and Pierre Le Doussal²

¹Dipartimento di Fisica dell'Università di Pisa and INFN, Pisa, Italy

² CNRS-Laboratoire de Physique Theorique de l'Ecole Normale Supérieure, 24 rue Lhomond, 75231 Paris, France

Abstract. We study the time evolution of quantum one-dimensional gapless systems evolving from initial states with a domain-wall. We generalize the path-integral imaginary time approach that together with boundary conformal field theory allows to derive the time and space dependence of general correlation functions. The latter are explicitly obtained for the Ising universality class, and the typical behavior of one- and two-point functions is derived for the general case. Possible connections with the stochastic Loewner evolution are discussed and explicit results for one-point time dependent averages are obtained for generic κ for boundary conditions corresponding to SLE. We use this set of results to predict the time evolution of the entanglement entropy and obtain the universal constant shift due to the presence of a domain wall in the initial state.

1. Introduction

The experimental realization of trapped quasi-one-dimensional atomic gases during the last few years [1, 2, 3, 4, 5, 6, 7, 8, 9] has provided a new impetus for the study of the effects of strong correlations on the physical properties of fundamental quantum mechanical systems of interacting particles. One very interesting aspect of this still emerging field, in contrast to traditional condensed matter physics, is that it is possible to follow the unitary time evolution in the absence of any dissipation [10, 11, 12, 13, 14, 15, 16].

The absence of a general theoretical framework to investigate the non-equilibrium dynamics of extended quantum systems led to the study of many one-dimensional models whose dynamics can be solved exactly (see e.g. Refs. [17, 18, 19, 20, 21, 22, 23, 24, 25, 26, 27, 28, 29, 30, 31, 32, 33, 34, 35, 36, 37, 38, 39, 40, 41], but the list is far from being exhaustive) and inspired the developing of new numerical methods among which time-dependent density-matrix renormalization-group (DMRG) is the most successful [42], giving the first opportunity to investigate the out of equilibrium behavior also of non-integrable systems as e.g. in Refs. [21, 43, 44, 45, 46, 47, 48, 49, 50, 51].

From the study of specific models it is difficult to draw general conclusions on the non-equilibrium physics of quantum systems. Hence it is desirable to have frameworks that, at least in some relevant time windows, can give results valid for a large class of systems. In Refs. [24, 30] a method to tackle the time evolution after a quantum quench (i.e. a sudden change of a Hamiltonian parameter) has been proposed. Within this method the real-time path integral representation of a d -dimensional quantum system is reduced to the thermodynamics of a $d + 1$ dimensional classical system in a slab geometry. The time translation invariance is explicitly broken by the initial state that plays the role of a boundary state in the slab. When the Hamiltonian H governing the time evolution is at or close to a quantum critical point, one can use the renormalization group (RG) theory of boundary critical phenomena (see e.g. [52]) to study the regime of time and length scales much larger than microscopic ones. In Refs. [24, 30] this approach has been mainly applied to the time evolution of one-dimensional (1D) systems since the 1+1 dimensional strip is described asymptotically by a boundary conformal field theory (CFT).

Two very intriguing properties were derived by using this approach. First, connected correlations start forming only after two points are causally connected (horizon effect). Second, the large time asymptotic of correlation functions are the same as in a thermal state with effective temperature $\beta_{\text{eff}} = 4\tau_0$ (τ_0 being related to the inverse of the mass gap in the initial state, see below), despite the fact that the system is always in a pure state. These predictions have been confirmed by a number of exact calculations in specific models. This path-integral approach is generalizable to several different situations and it is very surprising, despite the success in the simplest case, that this has been done only in a few cases (in Ref. [33] for the so called local quench and in Ref. [53] for the evolution of the order-parameter in higher dimensional systems).

In this paper we apply this imaginary time path-integral to the case in which the initial state is not translationally invariant but contains a domain-wall. We study the resulting time evolution governed by a gapless Hamiltonian using boundary CFT. A part from the per se interest, there are at least two additional reasons to study such an initial state. On one hand, the presence of a domain-wall generates a non-trivial transport, as shown by the exact solution in XX and XY chains [54]. On the other hand, in 2D classical critical systems, these are the typical boundary conditions used to set up the stochastic Loewner evolution (SLE), a mathematical rigorous approach to describe stochastic and geometric properties of 2D critical systems. Hence one must ask the question of whether SLE could be used to predict the time evolution of these quantum models.

The paper is organized as follows. In Sec. 2 we review the imaginary-time path-integral approach to quantum quenches. We specifically show how to tackle the case of a domain-wall in the initial state by means of CFT. In Sec. 3 we apply the method to the Ising model for which all the relevant correlation functions in the upper half-plane have been calculated in Ref. [55]. In Sec. 4 we describe which features of this quenches can be extracted by general CFT scaling without the knowledge of the full correlators in the upper half-plane and then in the following section 5 these results are used to

give prediction for the time-evolution of the entanglement entropy. In Sec. 6 we argue about possible connections with SLE and we discuss the case of two domain-walls in the initial state. Finally in Sec. 7 we critically discuss our findings and open problems. In Appendix A we report some useful formulas to perform the analytic continuations and in Appendix B we derive the time evolution for an homogeneous quench of the two-point functions of different operators.

2. The CFT approach to quantum quenches

In Refs. [24, 30] it has been shown how to extract from path-integral the unitary time-evolution of a d -dimensional system prepared in a state $|\psi_0\rangle$ that is not an eigenstate of H . The expectation value of a local operator $\mathcal{O}(\mathbf{r})$ at time t is

$$\langle \mathcal{O}(t, \mathbf{r}) \rangle = Z^{-1} \langle \psi_0 | e^{iHt - \epsilon H} \mathcal{O}(\mathbf{r}) e^{-iHt - \epsilon H} | \psi_0 \rangle, \quad (1)$$

where the damping factors $e^{-\epsilon H}$ have been introduced in order to make the path-integral representation of the expectation value absolutely convergent. $Z = \langle \psi_0 | e^{-2\epsilon H} | \psi_0 \rangle$ ensures that the expectation value of the identity is one. Eq. (1) may be represented by an analytically continued path integral in imaginary time, described by the evolution operator $e^{-(\tau_2 - \tau_1)H}$, which takes the boundary values ψ_0 on $\tau = \tau_1 = -\epsilon - it$ and on $\tau = \tau_2 = \epsilon - it$. The operator \mathcal{O} is inserted at $\tau = 0$. The width of the slab is 2ϵ . τ_1 and τ_2 must be considered as real numbers during all the calculation. Only at the end they are continued to their effective values $\pm\epsilon - it$. The real-time non-equilibrium evolution of a d dimensional system is then reduced to the thermodynamics of a $d + 1$ field theory in a slab geometry with the initial state $|\psi_0\rangle$ playing the role of boundary condition at both the borders of the slab. More generally the operator \mathcal{O} in Eq. (1) can depend on several points, and in the $d = 1$ case on which we focus below, we denote r_i the set of these points, together with possible domain-wall positions in the initial state.

We wish to study this setting in the limit where t and all separations $|r_i - r_j|$ are much larger than any microscopic length and time scales, so that renormalization group (RG) theory can be applied. If H is at or close to a quantum critical point, the bulk properties of the critical theory are described by a bulk RG fixed point (or some relevant perturbation thereof). Any *translationally invariant* boundary condition flows to one of a number of possible boundary fixed points [56, 57], and we may replace $|\psi_0\rangle$ by the appropriate RG-invariant boundary state $|\psi_0^*\rangle$ to which it flows. The difference may be taken into account by assuming that the RG-invariant boundary conditions are not imposed at $\tau = \tau_1$ and τ_2 but at $\tau = \tau_1 - \tau_0$ and $\tau = \tau_2 + \tau_0$. τ_0 is given by the absolute value of the extrapolation length and it characterizes the RG distance of the actual boundary state from the RG-invariant one [52]. In the quantum non-equilibrium problem, τ_0 is expected to be of the order of the correlation length in the initial state, that is the inverse energy gap [24, 30]. The effect of introducing τ_0 is simply to replace ϵ by $\epsilon + \tau_0$. The limit $\epsilon \rightarrow 0^+$ can now safely be taken, so the effective width of the slab results to be $2\tau_0$. For simplicity in the calculations, in the following we will consider the equivalent slab geometry between $\tau = 0$ and $\tau = 2\tau_0$ with the operator \mathcal{O} inserted at $\tau = \tau_0 + it$.

If the initial condition (and so the boundary one in the imaginary time representation) is not translational invariant, the approach must be changed accordingly. For example, in Ref. [33] it has been shown how to deal with initial conditions corresponding to the joining of two semi-infinite ground-states of a critical Hamiltonian. The case of domain-walls in the initial states, in which we are interested in this paper, is also easily tackled with boundary CFT. In fact, as shown by Cardy [56], any domain-wall at some position r_i can be viewed as the insertion of an appropriate operator Φ_{ab} at position r_i . The label a stands for the boundary condition to the right, and b to the left of the domain-wall respectively. Φ_{ab} is called *boundary condition changing* operator for obvious reasons. For any bulk CFT, there are a number of possible boundary states and consequently a number of boundary condition changing operators between them that are classified and their scaling dimensions are known (see e.g. [56]) in the most relevant cases.

In the upper half-plane with a boundary condition having m domain-walls (including the point at ∞) on the real axis, any n -point function can be obtained in terms of a $(2n + m)$ -point correlation

of the n operators plus m boundary condition changing ones. The $2n$ comes from the bulk points and their images. Increasing n and m technical difficulties to get these correlations increase considerably. For this reason, we focus on one- and two-point functions with two domain-walls (one at ∞). The difficulty of this calculation corresponds to that of four- and six-point functions in the complex plane.

2.1. The general strategy by conformal mapping

To obtain the time-dependence of a correlation function evolving from a state with one domain-wall (let say at $r = 0$ for simplicity), we need to analytically continue the same correlation function calculated in a strip of width $2\tau_0$ with boundary condition changing operators at $r = 0$ on both the borders of the strip. The strip complex coordinate is $w = r + i\tau$ with $0 < \tau < 2\tau_0$. The operators needed for the correlation functions are then inserted at $\tau = \tau_0 + it$. This geometry is depicted on the left of figure 1. Note that we have set the sound velocity to unity.

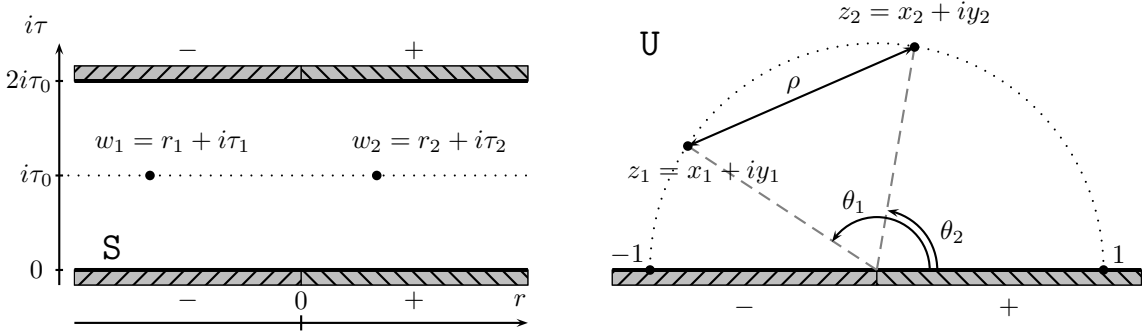


Figure 1. Left: Strip with domain-walls at $w = 0$ and $w = i2\tau_0$ and points at $r_i + i\tau$, with τ that must be analytically continued to $\tau_0 + it$. Right: Corresponding geometry on the upper half-plane after the mapping (2). For the two-point correlation functions, the Euclidean distance between the two points is given by $\rho^2 = (x_1 - x_2)^2 + (y_1 - y_2)^2$.

The strip geometry can be obtained by the conformal mapping of the upper half-plane $z = x + iy$ with a domain-wall in the origin (and one at ∞)

$$z = \frac{e^{\pi w/(2\tau_0)} - 1}{e^{\pi w/(2\tau_0)} + 1} = \tanh\left(\frac{\pi w}{4\tau_0}\right). \quad (2)$$

We indicate in all the paper the upper half-plane with \mathbf{U} and the strip with \mathbf{S} . θ is the argument of z in \mathbf{U} , as shown in figure 1 (right panel). Note that the conformal map used here is different from the one used in Refs. [24, 30] $w(z) = (2\tau_0/\pi) \ln z$ since we fix two marked points on the boundary (the two domain-walls).

In the case where \mathcal{O} is a product of local *primary* scalar operators $\Phi_i(w_i, \bar{w}_i)$, the expectation value in the strip is related to the one in \mathbf{U} by the standard transformation

$$\langle \prod_i \Phi_i(w_i, \bar{w}_i) \rangle_{\mathbf{S}} = \prod_i |w'(z_i)|^{-\Delta_i} \langle \prod_i \Phi_i(z_i, \bar{z}_i) \rangle_{\mathbf{U}}, \quad (3)$$

where $\Delta_i = 2h_i$ is the bulk scaling dimension of Φ_i . Often in the following we use the shorthand $\Phi_i(z)$ for $\Phi_i(z, \bar{z})$. Note that, as usual, when comparing to lattice models, an eventual expectation value of Φ_i in the ground state of H is supposed to have been subtracted off. The asymptotic real time dependence is obtained via the analytic continuation $\tau \rightarrow \tau_0 + it$, and taking the limit $t, r_{ij} \gg \tau_0$.

In the following sections we apply this method to several specific cases.

3. The Ising model

We start our analysis from the Ising model for which several correlation functions (of the two primary operators spin and energy) in the upper half-plane with a domain-wall have been already calculated by Burkhardt and Xue [55] (using specific results for four- and six-point correlation functions previously derived [58]). In the beginning, we shall focus our interest to domain-walls created by changing fixed boundary conditions from $a = +$ to $b = -$. We refer to this case as “ $+ -$ initial conditions”. The initial position of the domain wall is at $r = 0$ (unless noted otherwise) and a on its positive side. Then we separately discuss the case $a = +$ and $b = \text{free}$, a domain-wall defined via changing from fixed to free boundary conditions. We will abbreviate this case by “ $+f$ initial conditions”. All results here should be relevant for the time evolution of e.g. the Ising chain in a transverse field with Hamiltonian $H = -\frac{1}{2} \sum_i [s_i^x s_{i+1}^x + h s_i^z]$ (note that the state $|+\rangle$ here corresponds a spin aligned in the x direction). This model is easily diagonalized through a Jordan-Wigner transformation followed by a Bogoliubov rotation, that map it onto a free fermion lattice model (see e.g. appendix of Ref. [20]). It is critical at $h = 1$ and hence described there by a CFT with central charge $c = 1/2$.

3.1. $+ -$ initial condition: one-point functions

Spin. The σ expectation value with $+ -$ boundary condition in \mathbb{U} is [55]

$$\langle \sigma \rangle_{+-}^{\mathbb{U}} = \mathcal{A} \frac{\cos \theta}{y^{1/8}}, \quad (4)$$

where \mathcal{A} is a non-universal amplitude, that can be fixed in a universal way through the ratio with the amplitude of the bulk two-point function [59, 60] (but we will never use the explicit value of \mathcal{A}). This correlation function satisfies the correct (bulk) limiting behavior as $y \rightarrow +\infty$. Hence it is straightforward to read off that the scaling dimension of σ is $\Delta_\sigma = 2h_\sigma = 1/8$.

The magnetization profile in the strip with the central domain-wall is obtained by using Eq. (3) and the conformal mapping (2)

$$\langle \sigma \rangle_{+-}^{\mathbb{S}} = \mathcal{A} \sqrt{2} \left(\frac{\pi}{2\tau_0} \right)^{1/8} \frac{\sinh(\pi r/2\tau_0)}{(\cosh(\pi r/\tau_0) - \cos(\pi\tau/\tau_0))^{1/2}} \frac{1}{[\sin(\pi\tau/2\tau_0)]^{1/8}}. \quad (5)$$

To extract the real-time evolution we analytically continue to $\tau = \tau_0 + it$, obtaining (r stands for the distance from the domain-wall)

$$\langle \sigma(r, t) \rangle = \mathcal{A} \sqrt{2} \left(\frac{\pi}{2\tau_0} \right)^{1/8} \frac{\sinh(\pi r/2\tau_0)}{(\cosh(\pi r/\tau_0) + \cosh(\pi t/\tau_0))^{1/2}} \frac{1}{[\cosh(\pi t/2\tau_0)]^{1/8}}, \quad (6)$$

which for asymptotic large time and distances $\tau_0 \ll r, t$ reads

$$\langle \sigma(r, t) \rangle = \mathcal{A} \left(\frac{\pi}{\tau_0} \right)^{1/8} \text{sign}(r) \times \begin{cases} e^{-\pi t/16\tau_0} & t < |r|, \\ e^{-\pi t/16\tau_0} e^{-\pi(t-|r|)/2\tau_0} & t > |r|. \end{cases} \quad (7)$$

This result is depicted in the left panel of figure 2.

Let us now discuss and interpret this first result. It is the consequence of two competing effects:

- The states $+$ and $-$ are *not* eigenstates of the conformal Hamiltonian. Thus a half-line with $+$ (or $-$) initial condition evolves according to the results of Refs. [24, 30]. In particular, we expect $\langle \sigma(r, t) \rangle \propto e^{-\pi t/16\tau_0}$, that is nicely confirmed by Eq. (7) in the case $t < |r|$. Far enough from the origin, the system does not feel the domain-wall in the initial state and the exponential decay of the one-point function is the same as for a translational invariant initial state.
- The effect of the domain-wall (encoded in the first term of Eq. (6)) arrives at the point r only at time $t = |r|$ (we recall that the speed of sound has been set to 1) and it is responsible for an additional exponential time decay $e^{\pi(t-|r|)/2\tau_0}$. This can be seen as a result of the quantum averaging of spins with opposite orientations.

As usual [24, 30], the effect of finite τ_0 is only to smooth the time evolution close to the crossover point $t = |r|$.

Energy density. The time evolution of the energy-density operator can be obtained in analogous way. In the upper half-plane we have [55]

$$\langle \epsilon \rangle_{+-}^{\mathbb{U}} = \mathcal{B} \frac{4 \cos^2 \theta - 3}{y}, \quad (8)$$

i.e. the scaling dimension of ϵ is $\Delta_\epsilon = 2h_\epsilon = 1$ (as well known for Ising) and there is a different non-universal constant \mathcal{B} . Conformal mapping to the strip and the analytic continuation is worked out using the formulas in Appendix A. For $t, r \gg \tau_0$, we obtain

$$\langle \epsilon(r, t) \rangle \stackrel{t, r \gg \tau_0}{\cong} \mathcal{B} \left(\frac{\pi}{\tau_0} \right) e^{-\pi t / 2\tau_0} \times \begin{cases} 1 & t < |r|, \\ -3 & t > |r|. \end{cases} \quad (9)$$

See figure 2 (right) for illustration. The interpretation of the result is similar to the previous case, except that, contrary to the spin operator, the energy density of the $+$ and $-$ state are equal and so the result is symmetric with respect to the axis $r = 0$. For $t < |r|$, the time evolution is the same as in the absence of the domain-wall that only plays a role for $t > |r|$. However, for the energy, the domain-wall has a drastic influence, because the averaging of spins with opposite direction changes abruptly (at least for $\tau_0 \ll t, |r|$) the value of the energy density.

A cartoon of the time evolution of the one-point functions, e.g. in the transverse field Ising chain, goes as follows. The initial domain-wall state undergoes a spin-flip process which locally looks like $| - + \rangle \rightarrow (| + + \rangle - | - - \rangle) / \sqrt{2}$. This process does not affect the two-site magnetization (in the x direction), but makes vanishing the single-site one, that before was maximum. Also the energetic balance is positive since the singlet state has lower energy than the product one in the critical Ising chain. Similar processes at later times $t > |r|$ are responsible for the negative local ϵ and the suppressed magnetization (as in Eq. (7) inside the causal-cone of the domain-wall). We stress that this is only a cartoon of what happens *locally* because the real-time evolved state is highly entangled on a global scale (see the section about entanglement entropy).

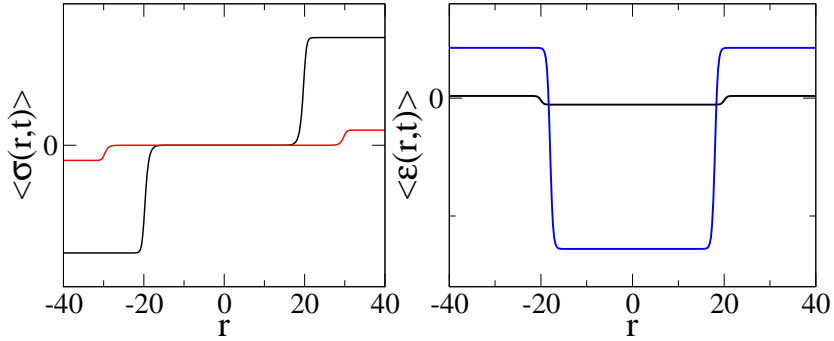


Figure 2. Space-time dependence of one-point correlation functions from a $+-$ initial condition. Left: $\langle \sigma(r, t) \rangle$ for $t = 20, 30$ as function of r . Right: $\langle \epsilon(r, t) \rangle$ for $t = 18, 20$ as function of r . Both the y axes are in arbitrary units and we fixed $\tau_0 = 1$.

3.2. $+-$ initial condition: two-point functions

Spin-spin. Let us start with the spin-spin correlation function. In the upper half-plane \mathbb{U} , we abbreviate $\sigma(z_k)$ with $z_k = x_k + iy_k$ by $\sigma(k)$, $k = 1, 2$. According to Ref. [55], for boundary conditions $+-$, as shown in figure 1, the two-point function is given by

$$\begin{aligned} \langle \sigma(1)\sigma(2) \rangle_{+-}^{\mathbb{U}} &= \frac{\mathcal{A}^2}{\sqrt{2}} \frac{1}{(y_1 y_2)^{1/8}} \left(\sqrt{u + u^{-1}} \cos \theta_1 \cos \theta_2 + \frac{u - u^{-1}}{\sqrt{u + u^{-1}}} \sin \theta_1 \sin \theta_2 \right) \\ &= \frac{\langle \sigma(1) \rangle_{+-}^{\mathbb{U}} \langle \sigma(2) \rangle_{+-}^{\mathbb{U}}}{\sqrt{2}} \sqrt{u + u^{-1}} \left(1 + \frac{u^2 - 1}{u^2 + 1} \tan \theta_1 \tan \theta_2 \right), \end{aligned} \quad (10)$$

with the same amplitude \mathcal{A} as for the one-point function. Here θ_i are polar angles as indicated in figure 1, and u an auxiliary variable defined via

$$u = \left(1 + \frac{4y_1y_2}{\rho^2}\right)^{1/4}. \quad (11)$$

Always using Eqs. (3) and (2) we obtain the strip result \mathbf{S}

$$\langle\sigma(1)\sigma(2)\rangle_{+-}^{\mathbf{S}} = \frac{\langle\sigma(1)\rangle_{+-}^{\mathbf{S}} \langle\sigma(2)\rangle_{+-}^{\mathbf{S}}}{\sqrt{2}} \sqrt{u+u^{-1}} \left(1 + \frac{u^2-1}{u^2+1} \frac{\sin(\pi\tau_1/2\tau_0) \sin(\pi\tau_2/2\tau_0)}{\sinh(\pi r_1/2\tau_0) \sinh(\pi r_2/2\tau_0)}\right), \quad (12)$$

where the Jacobians from conformal mapping have canceled out. The first factor does not contain any substantially new information since it is the product of two one-point functions. Analytic continuation of the various terms is performed in Appendix A. Putting everything together, we can write the time evolution of the two-point correlation function for $t, r_i, |r_1 - r_2| \gg \tau_0$ as

$$\langle\sigma(1)\sigma(2)\rangle = \begin{cases} \langle\sigma(1)\rangle\langle\sigma(2)\rangle & 2t < |r_1 - r_2|, \\ \frac{\langle\sigma(1)\rangle\langle\sigma(2)\rangle}{\sqrt{2}} e^{\pi(2t-|r_1-r_2|)/16\tau_0} \left(1 + s_1s_2 e^{\pi(2t-(|r_1|+|r_2|))/2\tau_0}\right) & 2t > |r_1 - r_2|, \end{cases} \quad (13)$$

with $s_i = \text{sign } r_i$, where $u \approx 1$ in the first regime and $u \rightarrow \infty$ in the second (since $2t < |r_1 - r_2| \leq |r_1| + |r_2|$ one can check from (A.10) that there is no third regime where small $u - 1$ terms could mix with a large contribution from the s_1s_2 term). This divides in different sub-regimes according to the relative values of $r_1, r_2, |r_1 - r_2|/2, t$. More precisely, we can distinguish two main regimes:

- $2t < |r_1 - r_2|$: the two points evolve independently since the horizon effect prevents from mutual interaction. The correlation decays as the product of the two one point functions and the connected correlation can be said to vanish (more precisely, its decay is subdominant). There are two possible sub-regimes:

$$\langle\sigma(1)\sigma(2)\rangle = \mathcal{A}^2 \left(\frac{\pi}{\tau_0}\right)^{1/4} s_1s_2 e^{-\pi t/8\tau_0} \times \begin{cases} 1 & t < \min(|r_1|, |r_2|), \\ e^{\pi(t-|r_2|)/2\tau_0} & t > |r_2|. \end{cases} \quad (14)$$

the second regime exists only if $|r_1 - r_2| > 2 \min(|r_1|, |r_2|)$ and we have written it in the case $|r_2| < |r_1|$ (we will adopt this convention in this subsection). Let us denote Ia and Ib these two subregimes.

- $2t > |r_1 - r_2|$: One has then the following possible sub-regimes (which we can denote IIa,b and c, respectively):

- For $|r_1 - r_2|/2 < t < |r_1|, |r_2|$ we find

$$\langle\sigma(1)\sigma(2)\rangle = \frac{\mathcal{A}^2}{\sqrt{2}} \left(\frac{\pi}{\tau_0}\right)^{1/4} e^{-\pi|r_1-r_2|/16\tau_0}. \quad (15)$$

This is a quasi-equilibrium regime. Both points have space-like separation to the domain-wall, but time-like to each other, hence they equilibrate as if no domain-wall was present. Obviously this regime exists only if the two points are on the same side of the domain-wall $s_1s_2 = 1$. It only exists for a finite time interval, as eventually the domain-wall influence will be felt.

- For $|r_2| < t < |r_1|$ we have

$$\langle\sigma(1)\sigma(2)\rangle = \frac{\mathcal{A}^2}{\sqrt{2}} \left(\frac{\pi}{\tau_0}\right)^{1/4} e^{-\pi|r_1-r_2|/16\tau_0} \times \begin{cases} s_1s_2 e^{-\pi(t-|r_2|)/2\tau_0} & 2t < |r_1| + |r_2|, \\ e^{\pi(t-|r_1|)/2\tau_0} & 2t > |r_1| + |r_2|, \end{cases} \quad (16)$$

with an intermediate regime when correlation again evolves in time. Its absolute value first decreases down to the minimal value $|\langle\sigma(1)\sigma(2)\rangle|_{\min} \propto e^{-\pi(|r_1-r_2|+4(|r_1|-|r_2|))/16\tau_0}$ reached at time $t = (|r_1| + |r_2|)/2$. After that time it increases again. In addition, if the points are on opposite side of the domain-wall, there is a sudden change in sign (i.e. on scale τ_0) of the correlation at time $t = (|r_1| + |r_2|)/2 = |r_1 - r_2|/2$ hence only the second (increasing) part of

this subregime exists. Note that although the absolute value vanishes on time scales smaller than τ_0 , it is possible to define a minimum value on scales much larger than τ_0 , as can be seen on the two bottom figures in Fig. 3.

- Very large times $2t > |r_1 - r_2|, 2|r_1|, 2|r_2|$, almost all terms cancel out and we may simplify to

$$\langle \sigma(1)\sigma(2) \rangle = \frac{\mathcal{A}^2}{\sqrt{2}} \left(\frac{\pi}{\tau_0} \right)^{1/4} e^{-\pi|r_1-r_2|/16\tau_0}, \quad (17)$$

i.e. the correlation function is the same as in a thermal state with an effective temperature $\beta_{\text{eff}} = 4\tau_0$ as in the case without the domain-wall: the system has “relaxed” it.

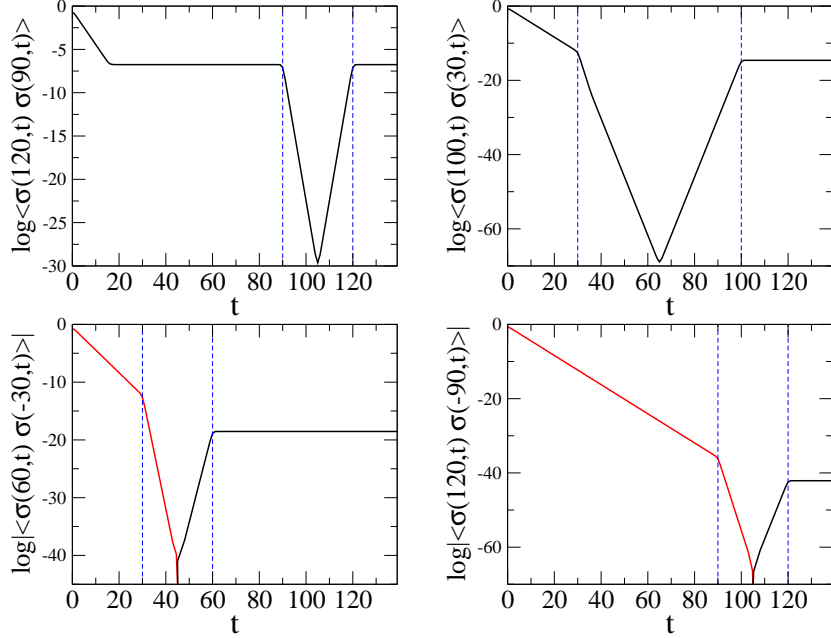


Figure 3. Two-point function of the spin operator for four different quenches with $(r_2, r_1) = (120, 90), (100, 30), (120, -90), (30, -60)$. They are the exact results with $\tau_0 = 1$. When a single r_j is negative ($r_j < 0$) we plot the absolute value. Signs are indicated by the colors of the curves: black corresponds to + and red to -.

Let us discuss these findings critically and describe which of these regimes are encountered as the system evolves. We start with the case of r_1 and r_2 on the same side of the domain-wall, i.e. without loss of generality $r_1 > r_2 > 0$. Then $r_1 - r_2 > 0$ can either be larger or smaller than $2r_2$. If $(r_1 - r_2)/2 < r_2$ then the evolution can be summarized as follow:

- $2t < r_1 - r_2$: the connected two-point function is constantly zero.
- $(r_1 - r_2)/2 < t < r_2$: the two-point function has a plateau at $e^{-\pi(r_1-r_2)/16\tau_0}$. Until this time the two points at r_1, r_2 did not yet feel the presence of the domain-wall. In fact the result is exactly the evolution found from a boundary state without domain-wall [24, 30], in analogy with the one-point functions.
- At $t = r_2$, the part of the system under consideration finally enters in the horizon of the domain-wall and the two-point function starts evolving again with an exponential decreasing up to the time $(r_1 + r_2)/2$. At this time, the correlation starts increasing toward the asymptotic value.
- At $t = r_1$ the system reaches its asymptotic value and the two point correlation does not evolve anymore. The domain-wall has been relaxed.

An example for $(r_1 - r_2)/2 < r_2$ is reported on the top left figure 3, where $(r_1, r_2) = (120, 90)$. The succession of regimes is thus Ia, IIa, IIb, IIc.

The case $2r_2 < r_1 - r_2$ turns out to be slightly different, and we give an example with $(r_1, r_2) = (100, 30)$ in the top right figure 3. In this case the sub-system feels the domain-wall before it is quasi-relaxed and so the succession of regimes is now Ia, Ib, IIb and IIc.

When the two points are on different sides of the domain-wall, clearly $|r_1 - r_2|/2$ (being the average of their absolute value) is always in between $|r_1|$ and $|r_2|$, so that the plateau (quasi-equilibrium) regime IIa never exists. Hence the succession of regimes is Ia, Ib, IIb (second half only) and IIc. Let us point out an interesting difference to the previous cases: for short time the two-point correlator is negative, since $s_1 s_2 = -1$, and changes sign at $t = |r_1 - r_2|/2$ (when the systems goes from regime Ib to IIb) in order to reach a positive asymptotic value. This can be easily understood: in fact for $2t < |r_1 - r_2|$ each point is out of the horizon of the other and evolves keeping its initial sign. Connected correlations start forming only after $t = |r_1 - r_2|/2$ when the two-point function changes sign.

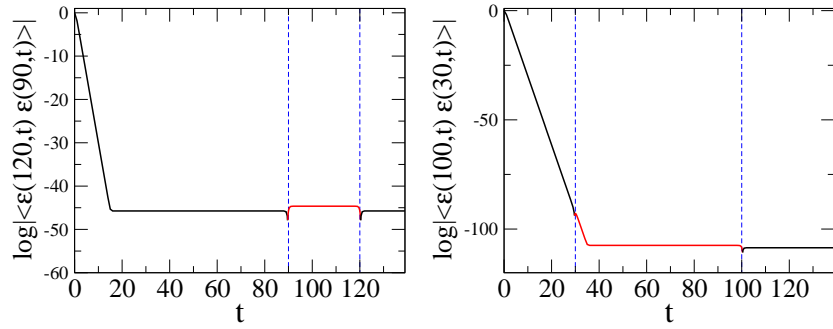


Figure 4. Absolute value of the energy-energy two-point function $\langle \epsilon(r_1, t) \epsilon(r_2, t) \rangle$ as a function of t for $(r_1, r_2) = (120, 90)$, and $(100, 30)$. We fix $\tau_0 = 1$. Signs are indicated by the colors of the curves: black corresponds to $+$ and red to $-$.

As a general conclusion, although the correlation reaches the same asymptotic large time equilibrium value as if the domain-wall was absent, we found that it does exhibit an interesting non-monotonic time dependence, which shows that the domain-wall has a disordering effect on the system at intermediate times. A complementary picture of the various regimes is given below (see Fig. 10).

Energy-energy. We proceed to the two-point function of the energy-density operator ϵ which has been calculated in Ref. [55] in the upper half-plane. We now map it to the strip and rewrite the resulting correlation function in a suitable way

$$\langle \epsilon(1) \epsilon(2) \rangle_{+-}^{\text{U}} = \langle \epsilon(1) \rangle_{+-}^{\text{U}} \langle \epsilon(2) \rangle_{+-}^{\text{U}} \times \left[1 + (u^4 - 1) \frac{1 - 4 \sin^2(\theta_1 - \theta_2)}{(1 - 4 \sin^2 \theta_1)(1 - 4 \sin^2 \theta_2)} - \frac{u^4 - 1}{u^4} \frac{1 - 4 \sin^2(\theta_1 + \theta_2)}{(1 - 4 \sin^2 \theta_1)(1 - 4 \sin^2 \theta_2)} \right]. \quad (18)$$

Transport to the strip is simple and the analytical continuation of the various terms is presented in Appendix A. Note that the factor $u^4 - 1$ indicates that the connected two-point function vanishes for $2t < |r_1 - r_2|$, as it can be seen from Eq. (A.10). As above, it corresponds to the independent evolutions of the two points, which are not yet causally connected. Hence we focus on $2t > |r_1 - r_2|$, when the two points interact. In this regime $u^4 \rightarrow \infty$ from Eq. (A.10) and one finds that only the second term in the parenthesis of Eq. (18) contributes. By analogy with the spin-spin correlation function, we find three different sub-regimes for $2t > |r_1 - r_2|$:

- (i) For $t > |r_1|, |r_2|$, the system displays thermal like correlations and, in fact, we find

$$\langle \epsilon(1) \epsilon(2) \rangle_{+-} = \mathcal{B}^2 \left(\frac{\pi}{\tau_0} \right)^2 e^{-\pi |r_1 - r_2| / 2 \tau_0}, \quad (19)$$

with the correct prefactor, and with $\beta_{\text{eff}} = 4\tau_0$ as it should be from general arguments (see below).

(ii) In the opposite limit $t < |r_1|, |r_2|$ (always with $2t > |r_1 - r_2|$), the correlation function is given by Eq. (19), with the *same* prefactor. The two points are quasi-equilibrated since they do not yet feel the presence of the domain-wall.

(iii) For $|r_2| < t < |r_1|$ (we assume without loss of generality $|r_1| > |r_2|$) we find

$$\langle \varepsilon(1)\varepsilon(2) \rangle_{+-} = -3\mathcal{B}^2 \left(\frac{\pi}{70} \right)^2 e^{-\pi|r_1-r_2|/2\tau_0}, \quad (20)$$

where the result is the same as in the other two regimes, only being multiplied by -3 . At variance from the spin correlation function, does not depend on time (apart from an obvious smoothing close to the changing times $t = |r_1|, |r_2|$). This apparently strange phenomenon, visible in Fig. 4, can be traced back to the fact that $\langle \varepsilon(r, t) \rangle$ for $t > |r|$ does not have any further exponential suppression, but only a discontinuity at $|r|$.

Spin-energy. In the upper half-plane \mathbb{U} , the spin-energy correlation function reads

$$\langle \sigma(1)\varepsilon(2) \rangle_{+-}^{\mathbb{U}} = \langle \sigma(1) \rangle_{+-}^{\mathbb{U}} \langle \varepsilon(2) \rangle_{+-}^{\mathbb{U}} \times \frac{1}{u^2} \left(\frac{u^4 + 1}{2} + (u^4 - 1) \frac{\tan \theta_1 \sin 2\theta_2}{4 \cos^2 \theta_2 - 3} \right). \quad (21)$$

The passage to the strip and the analytic continuation is easily done using formulae in Appendix A. Again for $2t < |r_1 - r_2|$ where $u \sim 1$, this two-point function is just the product of the one-point, in agreement with causality.

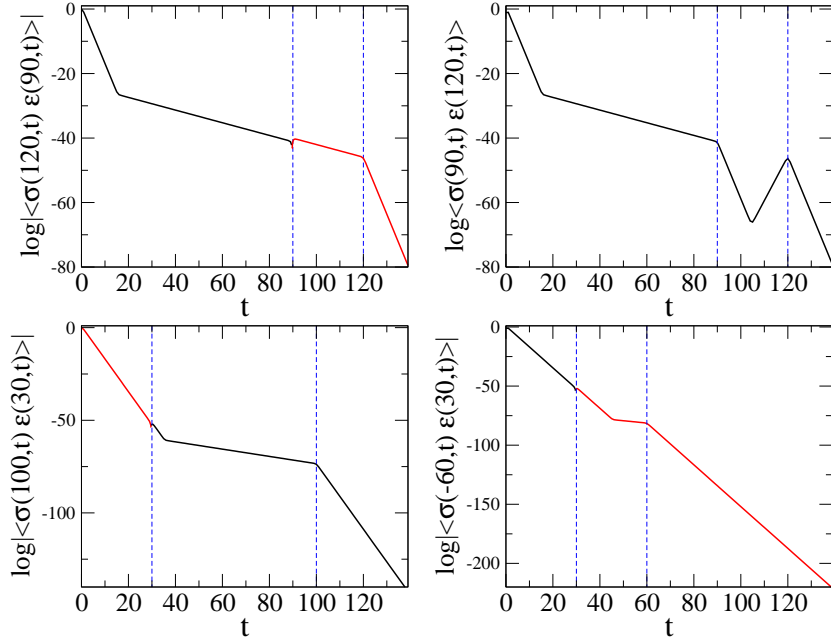


Figure 5. Absolute value of the spin-energy two-point functions $\langle \sigma(r_1, t)\varepsilon(r_2, t) \rangle$ as a function of t for $(r_1, r_2) = (120, 90), (90, 120), (100, 30)$, and $(-60, 30)$. We fix $\tau_0 = 1$. Signs are indicated by the colors of the curves: black corresponds to $+$ and red to $-$.

Slightly more involved is the opposite case $2t > |r_1 - r_2|$, where asymptotically we have

$$\langle \sigma(1)\varepsilon(2) \rangle_{+-} = \langle \sigma(1) \rangle_{+-} \langle \varepsilon(2) \rangle_{+-} e^{\pi(2t-|r_1-r_2|)/4\tau_0} \left(\frac{1}{2} + \frac{2s_1s_2e^{\pi(t-|r_1|)/2\tau_0}e^{-\pi|t-|r_2||/2\tau_0}}{1-4\Theta(t-|r_2|)} \right). \quad (22)$$

Here $\Theta(x)$ denotes the Heaviside function which is 1 for $x > 0$, and 0 otherwise. We will not give a detailed discussion of the various sub-regimes. Instead we give some examples in figure 5 where we illustrate the time evolution for several choices of r_1 and r_2 . Amongst the various cases, the most

interesting and new feature when compared to $\langle\sigma\sigma\rangle$ and $\langle\epsilon\epsilon\rangle$ is the very large time behavior: as t exceeds any other scale, i.e. for $t > |r_1|, |r_2|, |r_1 - r_2|/2$, we find that

$$\langle\sigma(1)\epsilon(2)\rangle_{+-} = 2\mathcal{A}\mathcal{B}s_2 e^{-\pi t(1/16+1/2)/\tau_0} e^{-(|r_1-r_2|-2|r_2|)/4\tau_0}, \quad (23)$$

which decays to zero for $t \rightarrow \infty$. Indeed this feature is in agreement with the well-known fact that the finite-temperature equilibrium value of a two-point function of operators with different scaling dimensions vanishes (see also Appendix B).

3.3. $+f$ initial condition: one-point functions

Let us consider different boundary conditions: we suppose a $+$ state on the half line from 0 to $+\infty$. On the negative real axis the spins are left free to take either value $+$ or $-$.

Spin. In the upper half-plane the one-point correlation function of the spin is [55]

$$\langle\sigma\rangle_{+f} = \mathcal{A}y^{-1/8}\sqrt{\cos(\theta/2)}. \quad (24)$$

Using results from Appendix A, the one-point function is asymptotically given by

$$\langle\sigma(r,t)\rangle_{+f} = \mathcal{A}\left(\frac{\pi}{\tau_0}\right)^{1/8} e^{-\pi t/16\tau_0} \begin{cases} 2^{-1/4} & |r| < t, \\ \Theta(r) & |r| > t. \end{cases} \quad (25)$$

See figure 6 (left panel) for an illustration. Note that the amplitude vanishes on the space like negative region $r < -t$ as for homogeneous free boundary conditions, and in fact matches the result of Eq. (7) on the space-like positive side $r > t$. Inside the time-like cone it takes a non trivial value.

Energy. In \mathbb{U} , the one-point function for the energy is [55]

$$\langle\epsilon\rangle_{+f} = \frac{\mathcal{B}}{y} \cos\theta, \quad (26)$$

that (a part the constant and the scaling dimension) is the same as the spin expectation value with $+-$ conditions and so we have the time evolution as

$$\langle\epsilon(r,t)\rangle_{+f} \simeq \mathcal{B}\left(\frac{\pi}{\tau_0}\right) e^{-\pi t/2\tau_0} \text{sign } r \begin{cases} e^{-\pi(t-|r|)/2\tau_0} & |r| < t, \\ 1 & |r| > t. \end{cases} \quad (27)$$

An illustration is given in figure 6 (right panel).

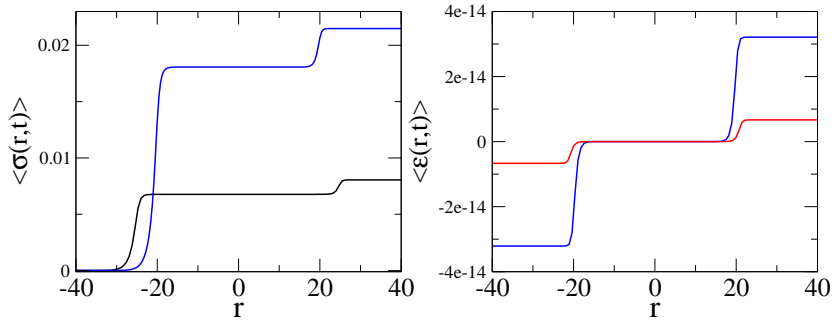


Figure 6. Left: One-point function $\langle\sigma(r,t)\rangle$ with $+f$ initial conditions for $t = 20$ (blue) and $t = 25$ (black). Right: One-point function $\langle\epsilon(r,t)\rangle$ for $t = 20$ (blue) and $t = 21$ (red). We fix $\tau_0 = 1$ and the y -axis are measured in arbitrary units.

3.4. $+f$ initial condition: two-point functions

Spin-spin. Again, Ref. [55] gives the half-plane result

$$\begin{aligned} \langle \sigma(1)\sigma(2) \rangle_{+f} &= \frac{\mathcal{A}^2}{\sqrt{2}} \frac{1}{(y_1 y_2)^{1/8}} \sqrt{(u + u^{-1}) \cos(\theta_1/2) \cos(\theta_2/2) + (u - u^{-1}) \sin(\theta_1/2) \sin(\theta_2/2)} \\ &= \frac{\langle \sigma(1) \rangle_{+f} \langle \sigma(2) \rangle_{+f}}{\sqrt{2}} \sqrt{u + u^{-1}} \sqrt{1 + \frac{u^2 - 1}{u^2 + 1} \tan(\theta_1/2) \tan(\theta_2/2)}. \end{aligned} \quad (28)$$

Relevant formulae for conformal mapping to the strip and analytic continuation are given in Appendix A. One finds similar regimes as for the $+ -$ initial conditions except that this two-point function is always positive, as a consequence of the non-negativity of one-point correlators. The main features are now standard. For time such that $2t < |r_1 - r_2|$ the two-point correlation function is just the product of the one-point ones, as $u \rightarrow 1$ in Eq. (28). For larger times, it is important to note that in the limit $u \rightarrow \infty$ one should be careful in using the second line in Eq. (28) because it has the form $0 \times \infty$. It is simpler to use the first line properly mapped to the strip (as explained in Appendix A) that is always finite. For times such that $2t > |r_1 - r_2|$ one finds, using that $u \rightarrow \infty$, a pseudo-thermal behavior with effective temperature $\beta_{\text{eff}} = 4\tau_0$, for all three possible subregimes (noted IIa,b,c above), with

$$\langle \sigma(r_1, t)\sigma(r_2, t) \rangle_{+f} = \frac{1}{\sqrt{2}} \mathcal{A}^2 \left(\frac{\pi}{\tau_0} \right)^{1/4} e^{-\pi|r_1 - r_2|/16\tau_0}, \quad (29)$$

for both small and large time regimes $t < |r_1|, |r_2|$ and $t > |r_1|, |r_2|$. More surprisingly one finds the same *time independent* result (29) for the intermediate time regime $|r_2| < t < |r_1|$, but with an amplitude multiplied by the factor $2^{-1/4}$. This is at variance with the behaviour of the $+ -$ case, and it is illustrated by two examples in figure 7, where two different pairs of values of r_1, r_2 are considered. We conclude that this kind of mixed domain-wall can be “dissipated” by the system, too.

The other two-point correlation functions with $(+f)$ boundary condition are known in the half-plane from Ref. [55]. We do not report their analysis here, since the main features of the Ising universality class are already present in the correlation reported so far. We rather highlight general features in the next section and show which information can be obtained from general scaling arguments only, without detailed knowledge of the full correlators.

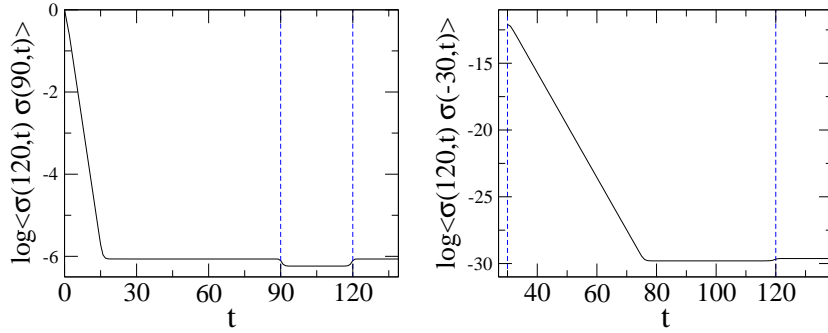


Figure 7. Spin-spin two-point functions $\langle \sigma(r_1, t)\sigma(r_2, t) \rangle_{+f}$ as a function of t for $(r_1, r_2) = (120, 90)$ (left) and $(120, -30)$ (right). We fix $\tau_0 = 1$. When at least one r is negative, the two-point function is practically zero outside the two causal cones.

4. General CFT results

Some of the results previously obtained for the Ising CFT with particular boundary conditions have a direct generalization to an arbitrary theory with any domain-wall in the initial state between two boundary conditions a (to its right) and b (to its left). In fact any n -point correlation

$(\zeta_1 - \zeta_2)^{-2\Delta_{ab}} \langle \Phi_1(z_1) \cdots \Phi_n(z_n) \rangle_{ab}^{\mathbb{U}}$ of primary operators satisfies the same differential equation as the full plane $2n + 2$ -point correlation $\langle \Phi_1(z_1) \Phi_1(\bar{z}_1) \cdots \Phi_n(z_n) \Phi_n(\bar{z}_n) \Phi_{ab}(\zeta_1) \Phi_{ab}(\zeta_2) \rangle$ and can be constructed from the same solutions, as discussed in full details in Ref. [55]. ζ_1 and ζ_2 stand for the start and end positions of the interface on the real axis, taken here to be $(0, \infty)$, and Δ_{ab} is the scaling dimension of the ab boundary changing operator Φ_{ab} . Let us discuss general consequences of this property.

The one-point function of any primary operator in the upper half-plane displays the scaling form

$$\langle \Phi(z) \rangle_{ab}^{\mathbb{U}} = \mathcal{A}_{aby}^{-\Delta_{\Phi}} f_{ab}^{\Phi}(\cos \theta), \quad (30)$$

where Δ_{Φ} is the scaling dimension of Φ and all the dependence on the boundary state is in $f_{ab}^{\Phi}(\cos \theta)$, with, as usual, $\cos \theta = x/(x^2 + y^2)^{1/2}$. In fact, $f_{ab}^{\Phi}(\cos \theta)$ explicitly depends on the boundary CFT and is related to hypergeometric functions of the corresponding full plane 4-point correlation.

A large class of primary operators displays a one-point function with a close analytic form (given in Ref. [55]), but in general they are quite complicated. However, from the previous examples, it is clear that we do not need the complete knowledge $f_{ab}^{\Phi}(\cos \theta)$ to understand the quench. Indeed upon mapping onto the strip and analytical continuation we already found

$$\cos \theta \rightarrow \text{sign } r \times \begin{cases} 1 & t < |r|, \\ e^{-\pi(t-|r|)/2\tau_0} & t > |r|. \end{cases} \quad (31)$$

Hence we need only the behavior for $\cos \theta \sim 0, \pm 1$. The case $\cos \theta \sim \pm 1$ means that in the upper half-plane the point z is far from the domain-wall and does not feel its effect. Consequently, $f(\cos \theta)$ takes the same value as for homogeneous boundary conditions a or b , related to $\cos \theta = 1$ and -1 respectively, with associated amplitudes $\mathcal{A}_{aa,bb} = \mathcal{A}_{ab} f_{ab}^{\Phi}(\pm 1)$. Conversely the case $\cos \theta = 0$ regards any point inside the causal cone of the domain-wall (i.e. causally connected within the speed of sound). The amplitude $f_{ab}^{\Phi}(0)$ can be either zero or finite, depending on the boundary CFT and the operator. We thus obtain

$$\langle \Phi(r, t) \rangle_{ab} = \mathcal{A}_{ab} \left(\frac{\pi}{\tau_0} \right)^{\Delta_{\Phi}} e^{-\pi t \Delta_{\Phi}/2\tau_0} \times \begin{cases} f_{ab}^{\Phi}(\pm 1) & t < |r|, \\ f_{ab}^{\Phi}(0) & t > |r|, \end{cases} \quad (32)$$

when $f_{ab}^{\Phi}(0) \neq 0$. Instead if $f_{ab}^{\Phi}(0) = 0$, the decay becomes faster, as $\sim e^{-\pi t \Delta_{\Phi}/2\tau_0 - \mu(\pi(t-|r|)/2\tau_0)}$ for $t > |r|$ if $f_{ab}^{\Phi}(\cos \theta) \sim \cos^{\mu} \theta$ around $\cos \theta = 0$, as in the case of the spin correlation with $+-$ boundary condition for the Ising model (with $\mu = 1$). An even more detailed discussion of the one-point functions is reported in Sec. 6 in connection with SLE. In particular we show explicitly in which cases $f_{ab}^{\Phi}(0)$ can vanish and that $f_{ab}^{\Phi}(\cos \theta)$ is analytic in zero, so in general $\mu = 1$.

The (relative) simplicity of these one-point function is related to the fact that bulk four-point functions can always be written as a general scaling part times a function of the unique cross-ratio of the four points. This is not the case for the two-point functions, which correspond to full plane six-point functions involving three independent cross ratios and the analysis is more complicated. However, we can give a general characterization. Considering a primary field Φ such that $\langle \Phi(z) \rangle \neq 0$, a scaling argument shows that we can always write the two-point function in \mathbb{U} with boundary condition ab as

$$\langle \Phi(z_1) \Phi(z_2) \rangle_{ab}^{\mathbb{U}} = \langle \Phi(z_1) \rangle_{ab}^{\mathbb{U}} \langle \Phi(z_2) \rangle_{ab}^{\mathbb{U}} F_{ab}^{\Phi}(u, \cos \theta_1, \cos \theta_2), \quad (33)$$

where the function F_{ab}^{Φ} is (to the best of our knowledge) unknown in the general case, and related to full-plane six-point functions. The variable u is defined in Eq. (11) is (one of the possible) cross ratio of $z_{1,2}$ and $\bar{z}_{1,2}$ (note that comparing with Ref. [30] one has $\eta \rightarrow 1$ for $u \rightarrow \infty$ and $\eta \rightarrow 0$ for $u \rightarrow 1$). Formula (33) still holds after mapping to the strip (replacing the index \mathbb{U} by \mathbb{S}) with the appropriate expressions for the variables u and $\cos \theta_i$ repeatedly used above and in Appendix A. We thus find that the interesting regimes for the time evolution are encoded in particular limits of F_{ab}^{Φ} . Namely:

- *Short times* $t < |r_1|, |r_2|$ and points on the same side of the initial domain-wall. In this case, depending on the signs of r_i , we have $\cos \theta_i = \pm 1$. This corresponds to two points extremely close to one boundary condition, i.e.

$$F_{ab}^\Phi(u, 1, 1) = F_{aa}(u), \quad F_{ab}^\Phi(u, -1, -1) = F_{bb}(u), \quad (34)$$

where $F_{aa}(u)$ ($F_{bb}(u)$) corresponds to the two-point scaling function with homogeneous a (b) boundary condition. In this case the problem reduces to the one evolving from homogeneous initial condition. Note that $\mathcal{A}_{aa}^2 F_{aa}(u) = (u^4/4)^{\Delta_\Phi}$ for $u \rightarrow \infty$ as one recovers the bulk behavior and, upon mapping to the strip, thermal like behavior in the subcase $t > |r_1 - r_2|/2$ (see also below).

- *Short times* $2t < |r_1 - r_2|$, *even on different sides*. In this case $u \sim 1$, i.e. the distance of the two points is much larger than the distance from the boundary and $F_{ab}^\Phi(1, \cos \theta_1, \cos \theta_2) = 1$, meaning that the correlation function evolves like the product of the one-point ones.
- *Larger times* $2t > |r_1 - r_2|$, the points are causally connected and $u = e^{\pi(2t - |r_1 - r_2|)/8\tau_0} \gg 1$. Scaling requires that $F_{ab}^\Phi(u, \eta_1, \eta_2) = u^{4\Delta_\Phi} \phi_{ab}^\Phi(\eta_1, \eta_2)$ in this large u limit, so that the time dependence factorizes in front and

$$\langle \Phi(r_1, t) \Phi(r_2, t) \rangle_{ab} = \mathcal{A}_{ab}^2 \left(\frac{\pi}{\tau_0} \right)^{2\Delta_\Phi} e^{-\pi\Delta_\Phi|r_1 - r_2|/(2\tau_0)} f_{ab}^\Phi(\eta_1) f_{ab}^\Phi(\eta_2) \phi_{ab}^\Phi(\eta_1, \eta_2). \quad (35)$$

The very large time subregime $t > |r_1|, |r_2|$ corresponds to $\eta_i = \cos \theta_i = 0$. Consequently, in \mathbb{U} the two points are deep in the bulk and give the bulk two-point function, leading to the thermal-like behavior. The other sub-regimes, when t is in between the various ‘‘critical’’ times $|r_i|$ can be extracted from (35) by considering the limits $\cos \theta_i \rightarrow \pm 1, 0$ and may lead to additional time dependence. Note that $\mathcal{A}_{ab}^2 f_{ab}^\Phi(\eta_1) f_{ab}^\Phi(\eta_2) \phi_{ab}^\Phi(\eta_1, \eta_2) \rightarrow 4^{-\Delta_\Phi}$ as $(\eta_1, \eta_2) \rightarrow (1, 1)$ or $(-1, -1)$.

The same reasoning can be applied to any n -point correlation function: for short times all the points evolve incoherently, whereas for very long times the correlation function is the same as in a thermal state at the effective temperature $\beta_{\text{eff}} = 4\tau_0$. As for the homogeneous quench [30] it is easy to understand the technical reason that gives the effective temperature $4\tau_0$ both for asymptotic large times and also in the intermediate regime. As usual, finite temperature correlations can be calculated by studying the field theory on a cylinder of circumference $\beta = 1/T$. In CFT a cylinder is usually obtained by mapping the complex plane with the logarithmic transformation $w = \beta/(2\pi) \log z$, but one can equivalently use the inverse of Eq. (2) $w = \beta/\pi \arctanh z$ that differs from the logarithm for a mapping of the real axis. The form for the two-point function of a primary operator in the strip depends in general on the function $F(u, \cos \theta_i)$, but when we analytically continue, we find that $u \rightarrow \infty$, i.e. the original points in \mathbb{U} effectively are far from the boundary (more precisely their relative distance is much less than the distance from the real axis). Thus we get the same result as we would get if we conformally transformed from the full plane to a cylinder, and from the comparison of the two transformation the effective temperature is $\beta_{\text{eff}} = 4\tau_0$. The same argument is easily worked out for the multi-point functions.

5. The entanglement entropy

Entanglement is a central concept in quantum information science. Moreover it is becoming a common tool to study and analyze extended quantum systems because of its ability in detecting the scaling behavior close to a quantum critical point [61]. A powerful measure is the block entanglement entropy defined as follows. If the system is in a pure quantum state $|\Psi\rangle$, $\rho = |\Psi\rangle\langle\Psi|$ is the density matrix. Indicating with A a spatial subset of the system (such as a finite subset of spins in a spin chain) and with $\rho_A = \text{Tr}_B \rho$ the reduced density matrix of the subset A , the entanglement entropy is just the corresponding Von Neumann entropy

$$S_A = -\text{Tr}_A \rho_A \ln \rho_A, \quad (36)$$

and analogously for S_B . When ρ corresponds to a pure quantum state, S_A gives a measure of the amount of quantum correlation between A and B , and one can prove that $S_A = S_B$.

S_A can be calculated in a quantum field theory through the replica trick [62]

$$S_A = -\frac{\partial}{\partial n} \text{Tr} \rho_A^n \Big|_{n=1}. \quad (37)$$

This is particularly useful in CFT because, when A consists of disjoint intervals with N boundary points with B we have that $\text{Tr} \rho_A^n$ transforms under a general conformal transformation as the N point function of a primary field Φ_n with conformal dimension [62] $\Delta_n = c/12(n-1/n)$, where c denotes the central charge of the underlying CFT. The fields Φ_n are usually called twist operators. In particular this implies that the entanglement entropy of a slit of length ℓ in an infinite system is given by [63, 62]

$$\text{Tr} \rho_A^n = c_n \left(\frac{\ell}{a}\right)^{-2\Delta_n} \Rightarrow S_A = \frac{c}{3} \log \frac{\ell}{a} - c'_1, \quad (38)$$

where a is an UV cutoff (e.g. in a spin chain is the lattice spacing) and c'_1 a non universal constant.

Clearly within this mapping to correlation function we can calculate the time-dependence of the entanglement entropy. For the case of homogenous quenches this has been done in Ref. [20], finding

$$S_A(t) \simeq \begin{cases} \frac{\pi ct}{6\tau_0} & t < \ell/2, \\ \frac{\pi c \ell}{12\tau_0} & t > \ell/2. \end{cases} \quad (39)$$

This result can be easily explained in terms of the causal scenario longly discussed there, and it is due to pairs of coherent quasi-particles emitted from any point and reaching one the subsystem A and the other B . In the case of A and B corresponding to two semi-infinite lines is a straightforward generalization of the previous result. In fact, we have only to consider the one-point correlation function of a twist operator $\langle \Phi_n \rangle$ that in the upper half-plane is $\langle \Phi_n(z, \bar{z}) \rangle_U = \tilde{c}_n [\text{Im}z]^{-\Delta_n}$ (where \tilde{c}_n is the analogous of c_n for the boundary CFT introduced in [62]). Mapping to the strip, analytically continuing, and taking the limit of large time, directly gives that the entanglement entropy grows indefinitely with time as $S_A(t) = \pi ct/12\tau_0$. Let us mention that this indefinite grow of entanglement is the main reason why numerical simulations (e.g. à la density matrix renormalization group) do not perform efficiently for this kind of time evolution [64].

The natural question arising is how this result is modified by the presence of the domain-wall at $r = 0$. Let us start with the case of two semi-infinite lines with $A = [r, \infty)$ and $B = \mathbb{R} \setminus A$ its complement. In this case the entanglement is given by the one-point function $\langle \Phi_n(r, t) \rangle$ of a twist operator at position r . From the general result reported above Eq. (32), we know that $S_A(t)$ increases linearly with time for $t < |r|$, as expected because the time evolution is the same as in the absence of the domain-wall. For $t > |r|$ we also find from Eq. (32) a linear increase of the entropy, but its rate in principle could change if $f_{ab}^{\Phi_n}(0)$ is vanishing. However, the properties $\Delta_1 = 1$ and $\text{Tr} \rho = 1$ trivially leads to $\mathcal{A}_{ab} f_{ab}^{\Phi_1}(0) = 1$. Analyticity in n and $\cos \theta$ near zero makes then $f_{ab}^{\Phi_n}(\cos \theta \rightarrow 0)$ non zero close to $n = 1$ and this ensures that the domain-wall does not change the linear increasing rate of the entanglement entropy, but only changes it up to an additive constant. The finite change, with respect to e.g. a homogeneous initial conditions of type a , is given by $\mathcal{S}_{ab} = -\partial_n (\mathcal{A}_{ab} (f_{ab}^{\Phi_n}(0) - f_{ab}^{\Phi_n}(1)))|_{n=1}$, independent of r with $|r| < t$. Hence the entanglement of the two parts being initially separated by the domain-wall increases linearly with only a *universal additive constant* \mathcal{S}_{ab} distinguishing from the homogeneous quench. This constant is computed below, in the particular cases relevant for SLE.

For the entanglement entropy of a finite slit $A = [r_1, r_2]$ with $\ell = |r_1 - r_2|$, general features are simple consequences of the scaling form in Eq. (33). As long as $t < |r_1|, |r_2|$, the time evolution remains the same as in the absence of the domain-wall (i.e. initial linear increase and then saturation). Conversely for large times $t > |r_1|, |r_2|, \ell/2$ the entanglement entropy saturates to a value proportional to ℓ . In the intermediate regimes, that depend on the nature of the domain-wall, from the general scaling again only finite universal shifts compared to the homogeneous quench can be possible.

6. Connection with SLE

Geometrical and statistical properties of a two-dimensional critical system in the half-plane with an interface starting at the boundary are nowadays widely studied by means of the so called stochastic Loewner evolution (SLE) that allows for a rigorous mathematical derivation of some CFT results (see e.g. Refs. [65] as reviews). We do not enter here in the beautiful technical details of the approach, but we will limit to state some results and ask whether they may have some connection with the quench problem considered here. An SLE interface receives a CFT interpretation as being created by inserting a boundary changing operator Φ_{12} at the boundary. In some cases, such as Ising, it corresponds to a domain wall and an ab boundary change. Hence for simplicity we stick here to the Ising notations, keeping in mind that in this section we deal with boundary condition changes relevant for SLE_κ at generic value of the parameter κ . These may be quite different from Ising, and are detailed in e.g. Refs. [65].

One of the most celebrated result concerns the rigorous derivation of Schramm's formula [66]. Starting from the boundary the interface explores the full upper half-plane and ends at infinity. This curve (called the SLE trace) divides the half plane in two parts. Schramm's formula gives the probability that one point lies to the right of this curve. In the continuum limit, this probability only depends on the angle θ that the point makes with the boundary (that is the same θ we used in all the paper). Schramm's formula gives this probability as

$$p(\theta) = H(\cot \theta) = \frac{1}{2} + \frac{\Gamma(4/\kappa) \cot \theta}{\sqrt{\pi} \Gamma(4/\kappa - 1/2)} {}_2F_1 \left(\frac{1}{2}, \frac{4}{\kappa}, \frac{3}{2}; -\cot^2 \theta \right), \quad (40)$$

satisfying the ‘‘boundary conditions’’ $p(\theta = \pi/2) = 1/2$ (reflection symmetry) and $p(\theta = \pi) = 0$ (point at the negative real axis). The parameter κ is the diffusion constant of the underlying stochastic process and turns out to define different universality classes (e.g. the Ising model corresponds to $\kappa = 3$) and is related to the central charge.

Since SLE focuses on geometrical properties of interfaces, one could try to push the continuation to real time t , and define a space-time interface geometrically using the path integral formulation. This can be done in principle by appropriate continuum limit (in the time direction) of lattice models such that the interface remains well defined. Consider the Ising case as a typical example. Specifying an interface means specifying the local spins $+$ (to the left) and $-$ (to the right) along a simple curve in the r, t plane (since it wanders this entails creation and annihilation of domain-walls as t increases). One must then superpose the complex amplitudes associated with all configurations satisfying that dynamical constraint. These are continuations of the real positive probabilities used to construct SLE. Schramm's dimension zero operator additionally constraints the interface to pass right of a space time point (i.e. to be connected to one of the two boundary conditions a or b without crossing the interface). Clearly this qualitative picture needs to be made more concrete.

Can $p(\theta)$ be used to determine some properties of the quench problem studied here? In order to address this question, let us map $p(\theta)$ to the strip according to Eq. (2), and then perform the analytical continuation $\tau \rightarrow \tau_0 + it$. A simple calculation gives

$$p(r, t) = H \left(\cot \theta = \frac{\sinh(\pi r / 2\tau_0)}{\cosh(\pi t / (2\tau_0))} \right), \quad (41)$$

that is a positive number smaller than 1. Hence it could in principle still be interpreted as a probability. In the limit $t, |r| \gg \tau_0$, using the properties of the hypergeometric function, we find

$$p(r, t) \Big|_{|r|, t \gg \tau_0} \begin{cases} 0 & r < -t, \\ 1/2 & -t < r < t, \\ 1 & r > t, \end{cases} \quad (42)$$

independently from κ . This result is suggestive and could be thought, in a sense which remains to be made precise, as a probability of being in the state evolved from $+$, that is clearly zero for $r < -t$ and 1 for $r > t$. A plateau develops (see figure 8) for $r < |t|$ and by mirror symmetry it can here only take the value 1/2. It would be interesting to understand how this plateau forms from the path integral

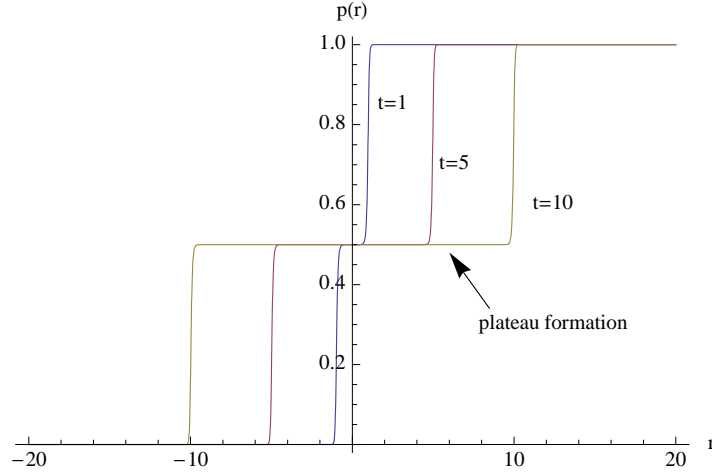


Figure 8. Probability $p(r, t)$ as given in Eq. (41) for different times t . Here, the parameters are $\tau_0 = 0.1$ and $\kappa = 3$ (Ising model). At large times, a plateau around $r = 0$ at $p = 1/2$ emerges.

formulation, presumably from interference effect. From the point of view of a real time relativistic theory it is however rather natural.

Are there other probabilities to which this could be compared? A priori the quantum state evolution is fully deterministic and apparently there is no probability into the game. A possible way to introduce a probability proceeds as follows. Consider, in a lattice model, the reduced density matrix $\rho_r(t)$ of the degrees of freedom localized in r (i.e. for a spin chain the spin in r). Clearly for $r > t$, $\rho_r(t)$ equals the analogous one obtained from the evolution of a homogenous + boundary condition $\rho_r^+(t)$. Analogously for $r < -t$, $\rho_r(t)$ is $\rho_r^-(t)$. An interesting possibility is that the reduced density matrix in the center region, $-r < t < r$, is simply a combination of the above two, in the present case by symmetry it can only be $\rho_r(t) = (\rho_r^-(t) + \rho_r^+(t))/2$. An interesting question then is whether the 1/2 found from Schramm's formula is the same factor appearing in front of the $\rho_r^+(t)$ reduced density matrix. It is easy to check in the Ising case, from our result for the averaged spin, that this could only hold strictly for infinite time (the leading decaying term in $e^{-\pi t/2\tau_0}$ does not agree). Unfortunately, in that limit, the factor 1/2 being imposed by symmetry does not provide a test. Tests would require more complicated situations, e.g. translating the results of Refs. [67, 68, 69] in terms of quantum evolution. For instance, in Ref. [67] the probability $P_{middle}(\cot \theta)$ was obtained, that a point z in the upper half plane lies in between (left of one, right of the other) two interfaces starting at nearby points on the real axis, *conditioned* to the fact they do not cross (i.e. going to infinity). This may be relevant to determine whether, in presence of *two* domain-walls in the initial state, e.g. an interval $[0, r_0]$ of – spins in an otherwise homogeneous + state, the point $r \gg r_0$ at time t still feels the presence of the – in the initial condition (however, this provides only part of the answer, since one should add the event where the domain-wall annihilates at late times, but this also can be obtained, in principle, within SLE). The large time continuation yields $P_{middle}(\cot \theta) \rightarrow D_\kappa$, the constant defined in Ref. [67], for all $t > |r|$, which has a non trivial value, e.g. $D_{\kappa=3} = 0.921866$ for Ising.

To close on a less speculative note, let us give the explicit form for the one-point function of any primary field of scaling dimension Δ in presence of the boundary conditions which are relevant for SLE. It is known that the boundary changing operator which creates an SLE_κ interface is Φ_{12} , with conformal dimension $\Delta_{12} = 2h_{12} = (6 - \kappa)/\kappa$. The result of Ref. [55] is then Eq. (32) with

$$f_{ab}(\cos \theta) = C_1 {}_2F_1(\alpha, \beta, 1/2, \cos^2 \theta) + C_2 \cos \theta {}_2F_1(\alpha + 1/2, \beta + 1/2, 3/2, \cos^2 \theta), \quad (43)$$

where for convenience we have absorbed the amplitude \mathcal{A}_{ab} into f_{ab} , with parameters

$$\alpha, \beta = \frac{1}{6} \left(1 - 2\Delta_{12} \pm [(1 - 2\Delta_{12})^2 + 12\Delta(1 + \Delta_{12})]^{1/2} \right) = (\kappa - 4 \pm \sqrt{(\kappa - 4)^2 + 8\kappa\Delta}) / (2\kappa). \quad (44)$$

We determine the constants C_1 and C_2 from the boundary conditions $f_{ab}(\pm 1)$ at $\theta = 0, \pi$ (respectively to the right/left of the domain-wall), that yields

$$C_1 = \frac{1}{2} \frac{f_{ab}(1) + f_{ab}(-1)}{{}_2F_1(\alpha, \beta, 1/2, 1)}, \quad C_2 = \frac{1}{2} \frac{f_{ab}(1) - f_{ab}(-1)}{{}_2F_1(\alpha + 1/2, \beta + 1/2, 3/2, 1)}. \quad (45)$$

Using the identity ${}_2F_1(a, b, c, 1) = \Gamma(c)\Gamma(c-a-b)/(\Gamma(c-a)\Gamma(c-b))$, we find $c-a-b = (8-\kappa)/2\kappa$. Hence both denominators are finite for $0 < \kappa < 8$ (the denominator associated to C_1 equals 1 for all κ for $\Delta = 0$ and this is consistent with the result for the twist operators with $\Delta_1 = 0$ in the entanglement entropy section). However we find that C_1 has a pole for $\Delta = \Delta_n^{(1)} = \frac{\kappa}{2} (n + \frac{1}{2}) (n + \frac{4}{\kappa} - \frac{1}{2})$ and C_2 for $\Delta_n^{(2)} = \frac{\kappa}{2} (n+1) (n + \frac{4}{\kappa})$ both for non-negative integer n (note that the latter vanishes for $\Delta = 2$ for all κ). Hence for such operators the symmetry must be imposed for the result to be meaningful. Obviously one recovers the Ising results Eqs. (4) and (8) for $\kappa = 3$ inserting respectively $\Delta = 1/8$ (spin) and $\Delta = 1$ (energy).

Using the continuation formula (31) one finds formally the large time asymptotics for $t > |r|$ is given by Eq. (30) with

$$\mathcal{A}_{ab} f_{ab}(0) \rightarrow C_1 + C_2 e^{-\pi(t-|r|)/2\tau_0} + \dots, \quad (46)$$

where the second decaying term becomes the leading one when $C_1 = 0$, else it is a rapidly decaying subleading correction.

Note that the Schramm formula is recovered, for some choice of boundary condition, considering an operator with scaling dimension $\Delta = 0$. One gets then $\beta = 0$ and $\alpha = 1 - 4/\kappa$ and

$$f_{ab}(\cos \theta) = C_1 + C_2 \cos \theta {}_2F_1(1/2, 3/2 - 4/\kappa, 3/2, \cos^2 \theta) = C_1 + C_2 \cot \theta {}_2F_1(1/2, 4/\kappa, 3/2, -\cot^2 \theta),$$

using properties of hypergeometric functions. It remains to be seen whether a dimension zero primary operator, relevant for the quench, can be identified. In that case it should be related to Schramm formula (or be trivial).

We can now compute, in the case of an SLE interface, the universal additive contribution \mathcal{S}_{ab} to the entanglement entropy as discussed in Section 5. Inserting $\Delta = c/12(n-1/n)$ which yields the appropriate values for α_n and β_n , and using the symmetry $f_{ab}^{\Phi_n}(-1) = f_{ab}^{\Phi_n}(1)$, we find

$$\mathcal{S}_{ab} = -\partial_n [{}_2F_1(\alpha_n, \beta_n, 1/2, 1)]^{-1}|_{n=1} = c \frac{\psi(\frac{4}{\kappa} - \frac{1}{2}) + \gamma_E + \ln 4}{3(\kappa - 4)}, \quad (47)$$

where $\psi(x)$ stands for the Polygamma function and, in terms of κ , the central charge is $c = (6-\kappa)(3\kappa-8)/(2\kappa)$. Notice that for $\kappa < 4$ (and in particular for the Ising model) this universal shift is negative.

6.1. Two domain-walls

Here we consider the case of two domain-walls in the initial state. It is more general, but in the context of SLE, it corresponds to a two interface problem and can be studied, for appropriate boundary conditions, by insertion of two Φ_{12} operators on each side in the strip. The corresponding strip geometry is depicted in Fig. 9. However, the complete correlation functions mapped on the upper half-plane need the insertion of four changing operators, that are in principle calculable but very cumbersome. To make progress, we first consider the limit of a small b domain in a line a when results can be obtained from the fusion of two Φ_{12} operators, which produces Φ_{13} operators. At the end, we finally argue that for asymptotic large time the result is valid for any finite fixed size domain b , not necessarily small. According to physical intuition this means that no matter how big is the b domain, it is always small compared to the infinite remaining a part.

Let us consider the operator $\mathcal{O} = \prod_i \Phi_i(w_i, \bar{w}_i)$ being a product of primary operators. When $|x_1 - x_2| = |x_3 - x_4| = \ell$ is small, taking into account the insertion of boundary condition changing

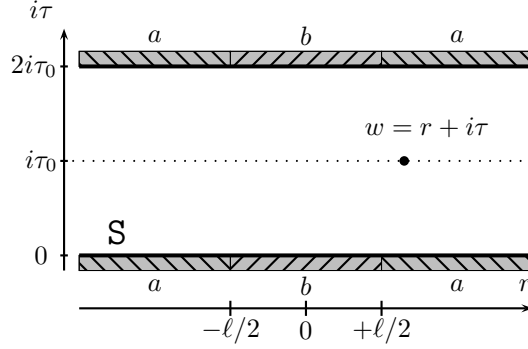


Figure 9. Strip geometry with domain-walls at $\pm\ell/2$ and $\pm\ell/2 + 2i\tau_0$.

operators, and the (generic) fusion algebra $\Phi_{12}\Phi_{12} \sim 1 + \Phi_{13}$, we obtain

$$\begin{aligned} \langle \mathcal{O} \rangle_{aba}^S &= \ell^{4\Delta_{12}} \left\langle \mathcal{O} \prod_{k=1}^4 \Phi_{12}(x_k) \right\rangle_S = \\ &= \langle \mathcal{O} \rangle_a^S + \ell^{\Delta_{13}} (\langle \mathcal{O} \Phi_{13}(0) \rangle_a^S + \langle \mathcal{O} \Phi_{13}(2i\tau_0) \rangle_a^S) + \ell^{2\Delta_{13}} \langle \mathcal{O} \Phi_{13}(0) \Phi_{13}(2i\tau_0) \rangle_a^S + \dots, \end{aligned} \quad (48)$$

where the dots denote the contribution of descendant operators, which are easily seen to include analytic $O(\ell^2)$ corrections as compared to the leading term which corresponds to homogeneous boundaries. The dimension of the Φ_{13} operator is, in the SLE context:

$$\Delta_{13} = \frac{8 - \kappa}{\kappa}. \quad (49)$$

In terms of SLE of each term in Eq. (48) can be interpreted as follows. The second term represents the contribution of two interfaces starting both very close to zero (respectively to $2i\tau_0$) on the same side of the strip and which do not immediately annihilate near their origin (but rather annihilate in the bulk). The last term corresponds to the possibility where the two interfaces cross the whole strip. It has thus some general relation to the calculation of Ref. [67], relation which can be made precise for a dimension zero operator. We recall here that we use Ising notations for convenience only but that we consider generic κ and the appropriate boundary changes [65]).

Let us now specialize to a single primary field $\mathcal{O} = \Phi(w)$ of conformal dimension Δ , being inserted at $w = r + i\tau$. As explained above, at the leading order in ℓ , these can be obtained simply from $\langle \Phi \rangle_a^S$, $\langle \Phi \Phi_{13}(0) \rangle_a^S$, and $\langle \Phi \Phi_{13}(0) \Phi_{13}(2i\tau_0) \rangle_a^S$. To calculate this one should map the result in the upper half-plane, that are obtained again by fusing two Φ_{12} . The calculations are straightforward. For example, applying a Moebius map to Eq. (30) one obtains the one point average in presence of a single finite domain, $\langle \Phi(z) \rangle_{aba}^U = \ell^{2\Delta_{12}} \langle \Phi(z) \Phi_{12}(0) \Phi_{12}(l) \rangle_U = y^{-\Delta} f_{ab}^\Phi(\cos \psi)$ with $\cos \psi = \text{Re}(\sqrt{z(l-\bar{z})}/\bar{z}(l-z))$ (the constant \mathcal{A}_{aba} is absorbed in f_{ab}^Φ again). This gives the lowest order terms in Eq. (48), with the correct amplitudes, from the expansion of $f_{ab}^\Phi(\eta = 1 - \zeta)/f_{ab}^\Phi(1) = 1 + C_a \zeta^{\Delta_{13}/2} + B_a \zeta + \dots$ for small $\zeta = \frac{1}{2}(\ell/y)^2 \sin^4 \theta + O(\ell^4)$. It yields in particular $\langle \Phi(z) \Phi_{13}(0) \rangle_U = C_a (\sin \theta)^{2\Delta_{13}} y^{-\Delta - \Delta_{13}}$. Putting everything together we finally obtain

$$\langle \Phi \rangle_{ababa}^U \sim \langle \Phi \rangle_a^U \left(1 + C_a \left(\frac{\ell}{y} \right)^{\Delta_{13}} (\sin \theta)^{2\Delta_{13}} + B_a \left(\frac{\ell}{y} \right)^2 (\sin \theta)^4 + \left(\frac{\ell}{y} \right)^{2\Delta_{13}} g^\Phi(\cos \theta) + \dots \right), \quad (50)$$

with $B_a = \alpha\beta/(1/2 + \alpha + \beta) = 4\Delta/(8 - 3\kappa)$ and $C_a = {}_2F_1(1/2 - \alpha, 1/2 - \beta, 1/2; 1)(C_1/f_{ab}(1)) + {}_2F_1(1 - \alpha, 1 - \beta, 3/2; 1)(C_2/f_{ab}(1))$, where C_1 and C_2 are given in (45), α, β in (44), and the relation given below (45) to ratio of Gamma function should be used to define the relevant limits. The general expression for the function $g^\Phi(\cos \theta)$ is given in Ref. [55] in terms of hypergeometric functions, using the fact that Φ_{13} being degenerate at level three, $\langle \Phi(z) \Phi_{13}(0) \Phi_{13}(\infty) \rangle_a^U$ obeys a simple differential equation. Note that the descendants will give non trivial corrections to (50), but these are always

subdominant to the leading correction and, quite often subdominant even to subleading ones. Hence in the general expansion in small (ℓ/y) at fixed $\cos\theta$, the leading correction comes from the $(\ell/y)^{\Delta_{13}}$ term only for $\Delta_{13} < 2$, i.e. for SLE type boundary conditions, $\kappa > 8/3$. For $\kappa < 8/3$ the B_a term dominates. Note however that even for $\kappa > 8/3$ the B_a term dominates if the amplitude vanishes $C_a = 0$. This is the case for the Ising model $\kappa = 3$ if Φ is either the bulk spin or energy operator, since $f_{ab}^{\Phi}(\eta)$ is analytic in these cases as discussed in Section 4. The last term is often subleading, although in principle there may be cases, for $\kappa > 4$, where C_a vanishes and the leading correction is given by the last term. Another example consists in the $O(n)$ loop model when each interface carries a different $O(n)$ index hence they cannot annihilate. The general case depend on the operator Φ , on the model, and on κ , and can be read from the above results.

Mapping to the strip and continuing to the real time quantum dynamics, we know that for $t > |r|$ the half plane variable $(\ell/y)\sin^2\theta$ in (50) maps to $\ell e^{-\pi(t-r)/2\tau_0}$, a variable which is small *both* in the small ℓ and the large time limit. Hence we find for large times $t > |r|$

$$\langle \Phi(r, t) \rangle_{aba} = \langle \Phi(r, t) \rangle_a (1 + C_a (\ell e^{-\pi(t-r)/2\tau_0})^{\Delta_{13}} + B_a \ell^2 e^{-\pi(t-r)/\tau_0} + \dots). \quad (51)$$

where one of the two correction terms dominates depending on whether Δ_{13} is larger or smaller than 2, and of whether C_a vanishes or not, as discussed above. The scaling variable governing the correction is then $\ell e^{-\pi t/2\tau_0}$, so no matter how large ℓ is, provided it is finite, for long times the leading correction is always of the above form. Physically this corresponds to the property that asymptotically the b domain is washed out and the time evolution is the same as from an homogeneous a initial condition with only exponentially small corrections. Although we have not attempted any calculation it is physically clear that any initial state with a local domain structure immersed in an infinite a initial state will behave in a similar fashion, possibly involving a spectrum of higher $\Delta_{1,2N+1}$ exponents, corresponding to $2N$ SLE curves. Applying to $\Delta \rightarrow \Delta_n$ and following the arguments of Section 5, one also easily sees that the difference in entanglement entropy as compared to the homogeneous case decays exponentially in time, with the same decay rates as in (51) and prefactors given by $-\partial_n(C_a, B_a)|_{n=1}$. Explicit calculation shows that the leading amplitude does not vanish. Similarly, in presence of an *odd* number of domain walls in a finite region in the initial state, the difference in entanglement entropy as compared to the homogeneous state, is expected to converge at large time, with similar exponentials, to the value of S_{ab} given by (47).

7. Conclusions

We presented a detailed study of the time evolution of a 1D quantum system evolving according to a gapless Hamiltonian from an initial state with one domain-wall. All our findings can be easily interpreted in terms of quasi-particles excitations emitted at time $t = 0$, and then propagating through the system at a finite speed given by the sound velocity $v_s = 1$. According to this scenario any correlation function has different time regimes. For example, in figure 10 the time evolution of the two-point correlation functions has different regimes resulting from the competition of the quasi-particles emitted from the middle point and those emitted from the domain-wall. The same interpretation is also valid for the entanglement entropy.

The importance of this simple physical picture is that it easily allows to understand limit and generality of the CFT results. In fact, the behavior outside the causal cones is only consequence of the finite velocity of sound and so it must be generally true also for gapped systems, as pointed out in details in Refs. [24, 30]. Oppositely, lattice models, even in the thermodynamic limit, have a full spectrum for the velocity of excitations, due to non-linear dispersion relations. These slow quasi-particle give corrections inside the causal cone to the results just derived (see Ref. [30] for a careful discussion of this issue).

As in the case of an homogeneous quench, we showed that for large times all the correlation functions are the same as in a thermal state with effective temperature $\beta_{\text{eff}} = 4\tau_0$. This means that the presence of the domain-wall does not affect the asymptotic state. In fact, this feature does not come unexpected since the energy of this state is only slightly larger than the translational invariant

one. Following this interpretation, we conclude that a state with an infinite number of domain-walls should change the effective temperature.

We finally discussed the possibility that the geometric picture obtained from SLE may be continued from imaginary to real time. Whether this may lead to new information for quantum quenches is not yet clear at this stage, but has been critically discussed in the present paper. We have also obtained, for the type of domain wall considered in SLE, the universal change in entanglement entropy as compared to an homogeneous initial state. Finally we considered the case of few domain walls in a finite region, and obtained the leading time decay of one point functions.

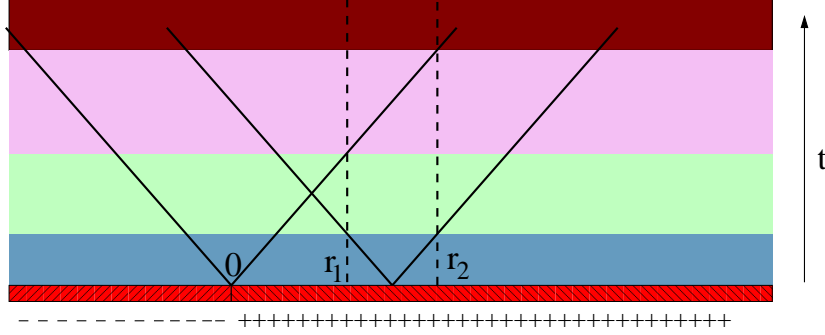


Figure 10. Causal interpretation of the results for all the two-point functions $\langle O(r_1, t)O(r_2, t) \rangle$. In the case shown with $(r_2 - r_1)/2 < r_1 < r_2$ and $r_i > 0$, there are four different time regimes, shown with different colors in the figure. 1) For $2t < r_2 - r_1$, the two points evolve independently (blue region). 2) For $(r_2 - r_1)/2 < t < r_1$, the two-point function is quasi stationary because there is not yet an influence of the domain-wall (green region). 3) For $r_1 < t < r_2$, the domain-wall enters in the dynamics (violet). 4) For $t > r_2$, stationary behavior with quasi-thermal correlations (red).

Acknowledgments

PC thanks John Cardy, Dragi Karevski, and Erik Tonni for useful discussions. This work has been done in part when PC was a guest of the Institute for Theoretical Physics of the Universiteit van Amsterdam (a stay supported by the ESF Exchange Grant 1311 of the INSTANS activity) and in part as guest at Ecole Normale Supérieure whose hospitality is kindly acknowledged. CH benefits from financial support from the French *Ministère de l'Éducation et de la Recherche* and PLD from ANR program 05-BLAN-0099-01.

Appendix A. Useful formulas for the analytic continuation

The strip geometry is obtained by the conformal mapping of the upper half-plane $z = x + iy$ to the strip $w = r + i\tau$ given by Eq. (2). It is useful to write it explicitly in cartesian and polar coordinate. We have

$$\begin{aligned}
 z &= \frac{e^{\pi w/(2\tau_0)} - 1}{e^{\pi w/(2\tau_0)} + 1} = \tanh\left(\frac{\pi w}{4\tau_0}\right), \\
 x &= \text{Re } z = \frac{\sinh(\pi r/2\tau_0)}{\cos(\pi\tau/2\tau_0) + \cosh(\pi r/2\tau_0)}, \\
 y &= \text{Im } z = \frac{\sin(\pi\tau/2\tau_0)}{\cos(\pi\tau/2\tau_0) + \cosh(\pi r/2\tau_0)}, \\
 |z|^2 &= \frac{\cosh(\pi r/\tau_0) - \cos(\pi\tau/\tau_0)}{2[\cos(\pi\tau/2\tau_0) + \cosh(\pi r/2\tau_0)]^2}.
 \end{aligned} \tag{A.1}$$

Upon continuation $\tau \rightarrow \tau_0 + it$ one has $\sin(\pi\tau/2\tau_0) \rightarrow \cosh(\pi t/(2\tau_0))$ and $\cos(\pi\tau/\tau_0) \rightarrow -\cosh(\pi t/\tau_0)$, but $\cos(\pi\tau/(2\tau_0))$ continues to an imaginary value. Hence the denominator must disappear in any

physical quantity, and it does, being compensated by the Jacobian

$$|z'(w)| = \frac{\pi}{4\tau_0} |1 - z(w)^2| = \frac{\pi}{2\tau_0 (\cos(\pi\tau/2\tau_0) + \cosh(\pi r/2\tau_0))} = y \frac{\pi/(2\tau_0)}{\sin(\pi\tau/2\tau_0)}. \quad (\text{A.2})$$

The polar angle θ is mapped to the strip according to

$$\cos \theta = \frac{x}{|z|} = \frac{\sqrt{2} \sinh(\pi r/2\tau_0)}{[\cosh(\pi r/\tau_0) - \cos(\pi\tau/\tau_0)]^{1/2}}, \quad \sin \theta = \frac{y}{|z|} = \frac{\sqrt{2} \sin(\pi\tau/2\tau_0)}{[\cosh(\pi r/\tau_0) - \cos(\pi\tau/\tau_0)]^{1/2}},$$

After analytic continuation we have

$$\cos \theta \rightarrow \frac{\sqrt{2} \sinh(\pi r/2\tau_0)}{[\cosh(\pi r/\tau_0) + \cosh(\pi t/\tau_0)]^{1/2}} \simeq \text{sign } r \times \begin{cases} 1 & t < |r|, \\ e^{-\pi(t-|r|)/2\tau_0} & t > |r|, \end{cases} \quad (\text{A.3})$$

$$\sin \theta \rightarrow \frac{\sqrt{2} \cosh(\pi t/2\tau_0)}{[\cosh(\pi r/\tau_0) + \cosh(\pi t/\tau_0)]^{1/2}} \simeq \begin{cases} e^{\pi(t-|r|)/2\tau_0} & t < |r|, \\ 1 & t > |r|. \end{cases} \quad (\text{A.3})$$

$$\tan \theta \rightarrow \frac{\cosh \pi t/2\tau_0}{\sinh \pi r/2\tau_0} \simeq \text{sign } r e^{\pi(t-|r|)/2\tau_0}, \quad (\text{A.4})$$

where here and in the following \simeq (and in the main text) stands for $t, r \gg \tau_0$.

We will also need the following functions of the angles that are trivially obtained from the previous formulae

$$\sin 2\theta = 2 \sin \theta \cos \theta \simeq 2 \text{sign } r e^{-\pi|t-|r||/2\tau_0}, \quad (\text{A.5})$$

$$\cos \frac{\theta}{2} = \left(\frac{1 + \cos \theta}{2} \right)^{1/2} \simeq \begin{cases} \Theta(r) & t < |r|, \\ 2^{-1/2} & t > |r|, \end{cases} \quad (\text{A.6})$$

$$\tan \frac{\theta}{2} = \sqrt{\frac{1 - \cos \theta}{1 + \cos \theta}} \simeq \begin{cases} 1 & t > |r|, \\ \frac{\Theta(-r)}{\Theta(r)} & t < |r|. \end{cases} \quad (\text{A.7})$$

$$4 \cos^2 \theta - 3 = \left(\frac{8 \sinh^2 \pi r/2\tau_0}{\cosh(\pi r/\tau_0) - \cos(\pi\tau/\tau_0)} - 3 \right) \simeq -1 + 2 \text{sign}(|r| - t) \quad (\text{A.8})$$

Here, $\Theta(r)$ denotes the Heaviside function which is 1 for $r > 0$, and 0 otherwise. Note the divergence for $r < -t$ in $\tan \theta/2$. However, this divergence cancels with the one-point function with free boundary condition and we do not need the first order correction in τ_0 that makes it finite.

For the two-point functions, we need to study the combination of different variables. In particular we need

$$u^4 = \left(1 + \frac{4y_1 y_2}{\rho^2} \right) = \frac{(x_1 - x_2)^2 + (y_1 + y_2)^2}{(x_1 - x_2)^2 + (y_1 - y_2)^2} = \frac{\cosh(\pi(r_1 - r_2)/2\tau_0) - \cos(\pi(\tau_1 + \tau_2)/2\tau_0)}{\cosh(\pi(r_1 - r_2)/2\tau_0) - \cos(\pi(\tau_1 - \tau_2)/2\tau_0)}, \quad (\text{A.9})$$

that is easily analytical continued to $\tau_{1/2} \rightarrow \tau_0 + it$ as

$$u^4 = 1 + \frac{\cosh^2(\pi t/2\tau_0)}{\cosh^2(\pi(r_1 - r_2)/4\tau_0)} = \begin{cases} 1 + e^{\pi(2t-|r_1-r_2|)/2\tau_0} \approx 1 & |r_1 - r_2| > 2t \gg \tau_0, \\ e^{\pi(2t-|r_1-r_2|)/2\tau_0} \gg 1 & 2t > |r_1 - r_2| \gg \tau_0. \end{cases} \quad (\text{A.10})$$

In particular all the terms like $(u^{2m} - 1)$ vanish for $2t < |r_1 - r_2|$ and the ratios $(u^{2m} - c_1)/(u^{2m} + c_2)$ tend to 1 for $2t > |r_1 - r_2|$, for all constants c_i .

For combinations of polar angles, we have

$$\sin(\theta_1 \pm \theta_2) = \sin \theta_1 \cos \theta_2 \pm \sin \theta_2 \cos \theta_1 \simeq \begin{cases} s_1 e^{-\pi(t-|r_1|)/2\tau_0} \pm s_2 e^{-\pi(t-|r_2|)/2\tau_0} & |r_1|, |r_2| < t, \\ s_2 \pm s_1 e^{-\pi(|r_2|-|r_1|)/2\tau_0} & |r_1| < t < |r_2|, \\ s_1 e^{\pi(t-|r_1|)/2\tau_0} \pm s_2 e^{\pi(t-|r_2|)/2\tau_0} & |r_1|, |r_2| > t, \end{cases}$$

$$\cos(\theta_1 \pm \theta_2) = \cos \theta_1 \cos \theta_2 \mp \sin \theta_2 \sin \theta_1 \simeq \begin{cases} s_1 s_2 e^{-\pi(t-|r_1|)/2\tau_0} e^{-\pi(t-|r_2|)/2\tau_0} \mp 1 & |r_1|, |r_2| < t, \\ s_1 s_2 e^{-\pi(t-|r_1|)/2\tau_0} \mp e^{\pi(t-|r_2|)/2\tau_0} & |r_1| < t < |r_2| \\ s_1 s_2 \mp e^{\pi(t-|r_1|)/2\tau_0} e^{\pi(t-|r_2|)/2\tau_0} & |r_1|, |r_2| > t, \end{cases}$$

where again $s_i = \text{sign } s_i$.

Appendix B. The two-point function of different operators in the quench from a homogeneous initial state

In Refs. [24, 30] it has been shown that when the initial state is a translation invariant state, the long-time correlation functions are the same as a pseudo-thermal state with $\beta_{\text{eff}} = 4\tau_0$. Then it follows that the correlation of operators with different scaling dimensions must vanish, but we still do not know how they fall off to zero. In this appendix we fill this small gap.

We first consider the energy-spin correlation in the Ising model starting from a homogeneous initial condition (we only consider fixed, since free boundary conditions gives σ correlation identically zero). In the upper half-plane \mathbb{U} the correlation function is [70]

$$\langle \sigma(1)\epsilon(2) \rangle_+^{\mathbb{U}} = \langle \sigma(1) \rangle_+^{\mathbb{U}} \langle \epsilon(2) \rangle_+^{\mathbb{U}} \frac{u^4 + 1}{2u^2}, \quad (\text{B.1})$$

where $\langle \sigma(1) \rangle_+^{\mathbb{U}} \propto y_1^{-1/8}$, and $\langle \epsilon(2) \rangle_+^{\mathbb{U}} \propto y_2^{-1}$, and u is defined as in (11) (see Appendix A for an explanation how to manipulate it). For $2t < |r_1 - r_2|$, we have $u \sim 1$ and the correlation function is the product of the one-point functions, in agreement with the causal interpretation. Oppositely when $2t > |r_1 - r_2|$, because $u^4 \sim e^{\pi(2t-|r_1-r_2|)/2\tau_0}$, we have

$$\langle \sigma(1)\epsilon(2) \rangle_+ \propto e^{-\pi t/16\tau_0} e^{-\pi t/2\tau_0} e^{\pi(2t-|r_1-r_2|)/4\tau_0} = e^{-\pi t/16\tau_0} e^{-\pi|r_1-r_2|/4\tau_0}, \quad (\text{B.2})$$

i.e. the two-point function is going to zero with an exponential rate.

Another simple example is the Gaussian model defined by the continuum Hamiltonian $H \propto \int_{y>0} (\nabla\phi(z))^2 dx dy$. The field ϕ is not primary, but its exponential $e^{i\alpha\phi(x)}$ with arbitrary α is primary with scaling dimension $\alpha^2/2$. The general correlation function is given by

$$\langle e^{i\alpha\phi(z_1)} e^{-i\beta\phi(z_2)} \rangle = e^{\alpha\beta G(z_1, z_2) - \alpha^2 G(z_1, z_1)/2 - \beta^2 G(z_2, z_2)/2}, \quad (\text{B.3})$$

with $G(z_1, z_2) = \langle \phi(z_1)\phi(z_2) \rangle$. Because of the restriction to the upper half-plane we have the Green function

$$G(z_1, z_2) = G_\infty(z_1 - z_2) - G_\infty(z_1 - \bar{z}_2) \quad (\text{B.4})$$

where $G_\infty(z) = G_\infty(0) - \log|z|$ is the Green function in the plane (we adsorbed the standard π factors in the definition of ϕ) and we assumed a fixed boundary condition (free ones are pathological because the one-point function is identically zero). We then have

$$\langle e^{i\alpha\phi(z_1)} e^{-i\beta\phi(z_2)} \rangle = \frac{1}{|z_{1\bar{1}}|^{\alpha^2/2} |z_{2\bar{2}}|^{\beta^2/2}} |z_{1\bar{2}}/z_{12}|^{\alpha\beta} \propto \frac{1}{y_1^{\alpha^2/2} y_2^{\beta^2/2}} u^{2\alpha\beta}. \quad (\text{B.5})$$

Using the previous formulas for the mapping to the strip and the analytic continuation we have for $2t < |r_1 - r_2|$ the independent evolution of the two points, while for $2t > |r_1 - r_2|$

$$\langle e^{i\alpha\phi(z_1, t)} e^{-i\beta\phi(z_2, t)} \rangle = e^{-\pi\alpha^2 t/4\tau_0} e^{-\pi\beta^2 t/4\tau_0} e^{\pi(2t-|r_1-r_2|)\alpha\beta/4\tau_0} = e^{-\pi(\alpha^2 + \beta^2 - 2\alpha\beta)t/4\tau_0} e^{-\pi\alpha\beta|r_1-r_2|/4\tau_0}, \quad (\text{B.6})$$

that always decays exponentially to zero because $(\alpha^2 + \beta^2 - 2\alpha\beta) > 0$.

It is easy to show that this indeed is a general feature of the homogeneous quench for different operators for any initial condition. In fact the, two-point function of different operators Φ_1 and Φ_2 in the upper half-plane can be always written as (when $\langle \Phi_1 \rangle \neq 0$ identically)

$$\langle \Phi_1(1)\Phi_2(2) \rangle^{\mathbb{U}} = \langle \Phi_1(1) \rangle^{\mathbb{U}} \langle \Phi_2(2) \rangle^{\mathbb{U}} F(u^4), \quad (\text{B.7})$$

where $F(u^4)$ can be related to the hypergeometric function determining the four-point functions in the bulk [71]. However its complete expression is not required: we only need the asymptotic behavior of $F(u^4 \simeq 1)$ and $F(u^4 \gg 1)$. From general scaling arguments, we have $F(1) = 1$ (i.e. close to the boundary the two-point function factorizes in one-points ones) and $F(u^4 \gg 1) \sim u^{-4x_b}$. The exponent x_b can be calculated for any pair of operators and any boundary condition from the bulk four-point functions [71]. Here, we only stress that if $\Phi_1 = \Phi_2$ then $x_b = x_1 = x_2$ to recover the right behavior of the bulk two-point function, and in general $x_b < (x_1 + x_2)/2$ for unitarity. Putting everything together we have

$$\langle \Phi_1(r_1, t) \Phi_2(r_2, 0) \rangle = \begin{cases} e^{-\pi x_1 t / 2\tau_0} e^{-\pi x_2 t / 2\tau_0} & 2t < |r_1 - r_2|, \\ e^{-\pi x_1 t / 2\tau_0} e^{-\pi x_2 t / 2\tau_0} e^{\pi x_b (2t - |r_1 - r_2|) / 2\tau_0} & 2t > |r_1 - r_2|. \end{cases} \quad (\text{B.8})$$

Note that when the operators Φ_1 and Φ_2 have the same scaling dimensions the time dependence disappear and we get the usual thermal like correlator. Oppositely, since $x_1 + x_2 - 2x_b > 0$, the correlation decays to zero as anticipated.

References

- [1] A. Görlitz, J. M. Vogels, A. E. Leanhardt, C. Raman, T. L. Gustavson, J. R. Abo-Shaeer, A. P. Chikkatur, S. Gupta, S. Inouye, T. Rosenband and W. Ketterle, Realization of Bose-Einstein Condensates in Lower Dimensions, *Phys. Rev. Lett.* **87**, 130402 (2001).
- [2] M. Greiner, I. Bloch, O. Mandel, T. W. Hänsch, and T. Esslinger, Exploring Phase Coherence in a 2D Lattice of Bose-Einstein Condensates, *Phys. Rev. Lett.* **87**, 160405 (2001) [cond-mat/0105105].
- [3] H. Moritz, T. Stöferle, M. Köhl, and T. Esslinger, Exciting Collective Oscillations in a Trapped 1D Gas, *Phys. Rev. Lett.* **91**, 250402 (2003) [cond-mat/0307607].
- [4] T. Stöferle, H. Moritz, C. Schori, M. Köhl, and T. Esslinger, Transition from a strongly interacting 1D superfluid to a Mott insulator, *Phys. Rev. Lett.* **92**, 130403 (2004) [cond-mat/0312440].
- [5] B. Paredes, A. Widera, V. Murg, O. Mandel, S. Falling, I. Cirac, G. V. Shlyapnikov, T. W. Hänsch, and I. Bloch, Tonks-Girardeau gas of ultracold atoms in an optical lattice, 2004 *Nature* **429**, 277.
- [6] T. Kinoshita, T. Wenger, and D. S. Weiss, Observation of a One-Dimensional Tonks-Girardeau Gas, 2004 *Science* **305**, 1125.
- [7] T. Kinoshita, T. Wenger and D. S. Weiss, Local Pair Correlations in One-Dimensional Bose Gases, *Phys. Rev. Lett.* **95**, 190406 (2005).
- [8] A. H. van Amerongen, J. J. van Es, P. Wicke, K. V. Kheruntsyan, and N. J. van Druten, Yang-Yang Thermodynamics on an Atom Chip, *Phys. Rev. Lett.* **100**, 090402 (2008) [0709.1899].
- [9] I. Bloch, J. Dalibard and W. Zwerger, Many-Body Physics with Ultracold Gases, *Rev. Mod. Phys.* to appear, [0704.3011].
- [10] M. Greiner, O. Mandel, T. W. Hänsch, and I. Bloch, Collapse and Revival of the Matter Wave Field of a Bose-Einstein Condensate, 2002 *Nature (London)* **419**, 51 [cond-mat/0207196].
- [11] C. Orzel, A. K. Tuchman, M. L. Fenselau, M. Yasuda, and M. A. Kasevich, Squeezed States in a Bose-Einstein Condensate, 2001 *Science* **291** 2386.
- [12] A. Widera, F. Gerbier, S. Fölling, T. Gericke, O. Mandel, and I. Bloch, Coherent Collisional Spin Dynamics in Optical Lattices, 2005 *Phys. Rev. Lett.* **95**, 190405.
- [13] L. E. Sadler, J. M. Higbie, S. R. Leslie, M. Vengalattore, and D. M. Stamper-Kurn, Spontaneous symmetry breaking in a quenched ferromagnetic spinor Bose-Einstein condensate, 2006 *Nature* **443**, 312.
- [14] T. Kinoshita, T. Wenger, and D. S. Weiss, A quantum Newton's cradle, 2006 *Nature* **440**, 900.
- [15] A. Widera, S. Trotzky, P. Cheinet, S. Fölling, F. Gerbier, I. Bloch, V. Gritsev, M. D. Lukin, and E. Demler, Quantum spin dynamics of squeezed Luttinger liquids in two-component atomic gases, 0709.2094.
- [16] S. Trotzky, P. Cheinet, S. Fölling, M. Feld, U. Schnorrberger, A. M. Rey, A. Polkovnikov, E. A. Demler, M. D. Lukin, and I. Bloch, Time-resolved Observation and Control of Superexchange Interactions with Ultracold Atoms in Optical Lattices, *Science* **319**, 285 (2008) [0712.1853].
- [17] L. Amico and A. Osterloh, Out of equilibrium correlation functions of quantum anisotropic XY models: one-particle excitations, 2004 *J. Phys. A* **37** 291 [cond-mat/0306285].
- [18] L. Amico, A. Osterloh, F. Plastina, R. Fazio, and G. M. Palma, Dynamics of Entanglement in One-Dimensional Spin Systems, 2004 *Phys. Rev. A* **69**, 022304 [quant-ph/0307048].
- [19] K. Sengupta, S. Powell, and S. Sachdev, Quench dynamics across quantum critical points, 2004 *Phys. Rev. A* **69** 053616 [cond-mat/0311355];
F. Igloi and H. Rieger, Long-Range Correlations in the Nonequilibrium Quantum Relaxation of a Spin Chain, 2000 *Phys. Rev. Lett.* **85** 3233 [cond-mat/0003193].
- [20] P. Calabrese and J. Cardy, Evolution of Entanglement entropy in one dimensional systems, *J. Stat. Mech.* P04010 (2005) [cond-mat/0503393].

- [21] G. De Chiara, S. Montangero, P. Calabrese, and R. Fazio, Entanglement Entropy dynamics in Heisenberg chains, 2006 J. Stat. Mech. P03001 [cond-mat/0512586].
- [22] R. W. Cherg and L. S. Levitov, Entropy and Correlation Functions of a Driven Quantum Spin Chain, 2006 Phys. Rev. A **73**, 043614 [cond-mat/0512689].
- [23] A. Minguzzi and D.M. Gangardt, Exact coherent states of a harmonically confined Tonks-Girardeau gas, 2005 Phys. Rev. Lett. **94**, 240404 [cond-mat/0504024].
- [24] P. Calabrese and J. Cardy, Time-dependence of correlation functions following a quantum quench, 2006 Phys. Rev. Lett. **96**, 136801 [cond-mat/0601225].
- [25] M. Rigol, V. Dunjko, V. Yurovsky, and M. Olshanii, Relaxation in a Completely Integrable Many-Body Quantum System: An Ab Initio Study of the Dynamics of the Highly Excited States of Lattice Hard-Core Bosons, 2007 Phys. Rev. Lett. **98**, 50405 [cond-mat/0604476].
- [26] M. A. Cazalilla. Effect of suddenly turning on the interactions in the Luttinger model, 2006 Phys. Rev. Lett. **97**, 156403 [cond-mat/0606236].
- [27] M. Rigol, A. Muramatsu, and M. Olshanii, Hard-core bosons on optical superlattices: Dynamics and relaxation in the superfluid and insulating regimes, 2006 Phys. Rev. A **74**, 053616 [cond-mat/0612415].
- [28] M. Cramer, C.M. Dawson, J. Eisert, and T.J. Osborne, Quenching, relaxation, and a central limit theorem for quantum lattice systems, Phys. Rev. Lett. **100**, 030602 (2008) [cond-mat/0703314].
- [29] V. Gritsev, E. Demler, M. Lukin, and A. Polkovnikov, Spectroscopy of Collective Excitations in Interacting Low-Dimensional Many-Body Systems Using Quench Dynamics, 2007 Phys. Rev. Lett. **99** 200404 [cond-mat/0702343].
- [30] P. Calabrese and J. Cardy, Quantum quenches in extended systems, J. Stat. Mech. P06008 (2007) [0704.1880].
- [31] V. Eisler and I. Peschel, Evolution of entanglement after a local quench, J. Stat. Mech. P06005 (2007) [cond-mat/0703379].
- [32] I. Klich, C. Lannert, and G. Refael, Supercurrent survival under Rosen-Zener quench of hard core bosons, Phys. Rev. Lett. **99**, 205303 (2007) [0706.2869].
- [33] P. Calabrese and J. Cardy, Entanglement and correlation functions following a local quench: a conformal field theory approach, J. Stat. Mech. P10004 (2007) [0708.3750].
- [34] M. Rigol, V. Dunjko, and M. Olshanii, Thermalization and its mechanism for generic isolated quantum systems, 0708.1324.
- [35] H. Buljan, R. Pezer, and T. Gasenzer, Fermi-Bose transformation for the time-dependent Lieb-Liniger gas, Phys. Rev. Lett. **100**, 080406 (2008) [0709.1444].
- [36] D. M. Gangardt and M. Pustilnik, Correlations in an expanding gas of hard-core bosons, 0709.2374.
- [37] V. Eisler, D. Karevski, T. Platini, I. Peschel, Entanglement evolution after connecting finite to infinite quantum chains, J. Stat. Mech. (2008) P01023 [0711.0289].
- [38] T. Barthel and U. Schollwoeck, Dephasing and the steady state in quantum many-particle systems, Phys. Rev. Lett. **100**, 100601 (2008) [0711.4896].
- [39] P. Barmettler, A. M. Rey, E. Demler, M. D. Lukin, I. Bloch, and V. Gritsev, Quantum Many-Body Dynamics of Coupled Double-Well Superlattices, 0803.1643.
- [40] W. H. Zurek, U. Dornier, and P. Zoller, Dynamics of a Quantum Phase Transition, 2005 Phys. Rev. Lett. **95** 105701 [cond-mat/0503511];
A. Polkovnikov, Universal adiabatic dynamics across a quantum critical point, 2005 Phys. Rev. B **72**, 161201(R) [cond-mat/0312144];
J. Dziarmaga, Dynamics of a quantum phase transition in the random Ising model, 2006 Phys. Rev. B **74**, 64416 [cond-mat/0603814];
L. Cincio, J. Dziarmaga, M. M. Rams, and W. H. Zurek, Entropy of entanglement and correlations induced by a quench: Dynamics of a quantum phase transition in the quantum Ising model, Phys. Rev. A **75**, 052321 (2007) [cond-mat/0701768];
T. Caneva, R. Fazio, G. E. Santoro, Adiabatic quantum dynamics of a random Ising chain across its quantum critical point, Phys. Rev. B **76**, 144427 (2007) [0706.1832];
K. Sengupta, D. Sen, and S. Mondal, Exact Results for Quench Dynamics and Defect Production in a Two-Dimensional Model, Phys. Rev. Lett. **100**, 077204 (2008) [0710.1712];
U. Divakaran and A. Dutta, The effect of the three-spin interaction and the next nearest neighbor interaction on the quenching dynamics of a transverse Ising model, J. Stat. Mech. (2007) P11001 [0801.0621];
F. Pellegrini, S. Montangero, G. E. Santoro, R. Fazio, Adiabatic quenches through an extended quantum critical region, 0801.4475;
S. Mondal, D. Sen, and K. Sengupta, Quench dynamics and defect production in the Kitaev and extended Kitaev models, 0802.3986.
- [41] V. Eisler and I. Peschel, Entanglement in a periodic quench, 0803.2655.
- [42] A. J. Daley, C. Kollath, U. Schollwoeck, and G. Vidal, Time-dependent density-matrix renormalization-group using adaptive effective Hilbert spaces, J. Stat. Mech. P04005 (2004) [cond-mat/0403313];
S. R. White and A. E. Feiguin, Real time evolution using the density matrix renormalization group, Phys. Rev. Lett. **93**, 076401 (2004) [cond-mat/0403310].
- [43] C. Kollath, U. Schollwoeck, J. von Delft, and W. Zwerger, One-dimensional density waves of ultracold bosons in an optical lattice, 2005 Phys. Rev. A **71**, 053606 [cond-mat/0411403].
- [44] C. Kollath, U. Schollwoeck, and W. Zwerger, Spin-charge separation in cold Fermi-gases: a real time analysis, 2005 Phys. Rev. Lett. **95**, 176401 [cond-mat/0504299].

- [45] C. Kollath, A. Laeuchli, and E. Altman, Quench dynamics and non equilibrium phase diagram of the Bose-Hubbard model, 2007 Phys. Rev. Lett. 98, 180601 [cond-mat/0607235].
- [46] K. Rodriguez, S.R. Manmana, M. Rigol, R.M. Noack, and A. Muramatsu, Coherent matter waves emerging from Mott-insulators, 2006 New J. Phys. **8**, 169 [cond-mat/0606155].
- [47] S.R. Manmana, S. Wessel, R.M. Noack, and A. Muramatsu, Strongly correlated fermions after a quantum quench, 2007 Phys. Rev. Lett. **98**, 210405 [cond-mat/0612030].
- [48] A. Kleine, C. Kollath, I. P. McCulloch, T. Giamarchi, U. Schollwoeck, Excitations in two-component Bose-gases, 0712.1448.
- [49] F. Heidrich-Meisner, M. Rigol, A. Muramatsu, A.E. Feiguin, and E. Dagotto, Ground-state reference systems for expanding correlated fermions in one dimension, Phys. Rev. Lett., to appear [0801.4454].
- [50] A. Laeuchli and C. Kollath, Spreading of correlations and entanglement after a quench in the Bose-Hubbard model, 0803.2947.
- [51] K. A. Al-Hassanieh, F. A. Reoredo, A. E. Feiguin, I. Gonzalez, and E. Dagotto, Excitons in the One-Dimensional Hubbard Model: a Real-Time Study, 0804.0617.
- [52] H. W. Diehl, The theory of boundary critical phenomena, in *Phase Transitions and Critical Phenomena* vol 10 ed C. Domb and J. L. Lebowitz (1986, London: Academic)
H. W. Diehl, The theory of boundary critical phenomena, Int. J. Mod. phys. B **11**, 3503 (1997) [cond-mat/9610143].
- [53] P. Calabrese and A. Gambassi, Quantum quench close to a critical point: Landau-Ginzburg order-parameter evolution, to appear.
- [54] T. Antal, Z. Racz, A. Rakos, and G. M. Schutz, Transport in the XX chain at zero temperature: Emergence of flat magnetization profiles, Phys. Rev. E **59**, 4912 (1999) [cond-mat/9812237];
D. Karevski, Scaling behaviour of the relaxation in quantum chains, Eur. Phys. J. B **27**, 147 (2001) [cond-mat/0203078];
Y. Ogata, Diffusion of the Magnetization Profile in the XX-model, Phys. Rev. E **66**, 066123 (2002) [cond-mat/0210011];
W. H. Aschbacher and C.-A. Pillet, Non-equilibrium steady states of the XY chain, J. Stat. Phys. **112**, 1153 (2003);
T. Platini and D. Karevski, Scaling and front dynamics in Ising quantum chains, Eur. Phys. J. B **48**, 225 (2005) [cond-mat/0509594];
W. H. Aschbacher and J.-M. Barbaroux, Out of equilibrium correlations in the XY chain, Lett. Math. Phys. **77**, 11 (2006);
T. Platini and D. Karevski, Relaxation in the XX quantum chain, J. Phys. A **40**, 1711 (2007) [cond-mat/0611673];
W. H. Aschbacher, Non-zero entropy density in the XY chain out of equilibrium, Lett. Math. Phys. **79**, 1 (2007).
- [55] T. W. Burkhardt and T. Xue, Conformal invariance and critical systems with mixed boundary conditions, Nucl. Phys. B **354**, 653 (1990);
T. W. Burkhardt and T. Xue, Density profiles in confined critical systems and conformal invariance, Phys. Rev. Lett. **66**, 895 (1991).
- [56] J. L. Cardy, Conformal Invariance and Surface Critical Behavior, 1984 Nucl. Phys. B **240** 514.
- [57] J. L. Cardy, Boundary Conformal Field Theory, in *Encyclopedia of Mathematical Physics*, ed J.-P. Francoise, G. Naber, and S. Tsun Tsou, (Elsevier, Amsterdam, 2006).
- [58] T. W. Burkhardt and I. Guim, Bulk, surface, and interface properties of the Ising model and conformal invariance, Phys. Rev. B **36**, 2080 (1987);
P. Di Francesco, H. Saleur, and J. B. Zuber, Critical Ising Correlation Functions In The Plane And On The Torus, Nucl. Phys. B **290**, 527 (1987).
- [59] J. L. Cardy, Effect of Boundary Conditions on the Operator Content of Two-Dimensional Conformally Invariant Theories. Nucl. Phys. B **275**, 200 (1986).
- [60] J. Cardy and D. Lewellen, Bulk and Boundary Operators in Conformal Field Theory, 1991 Phys. Lett. B **259** 274.
- [61] L. Amico, R. Fazio, A. Osterloh, and V. Vedral, Entanglement in Many-Body Systems, Rev. Mod. Phys. to appear [quant-ph/0703044].
- [62] P. Calabrese and J. Cardy, Entanglement entropy and quantum field theory, J. Stat. Mech. P06002 (2004) [hep-th/0405152]
- [63] C. Holzhey, F. Larsen, and F. Wilczek, Geometric and Renormalized Entropy in Conformal Field Theory, Nucl. Phys. B **424**, 443 (1994) [hep-th/9403108];
G. Vidal, J. I. Latorre, E. Rico, and A. Kitaev, Entanglement in quantum critical phenomena, Phys. Rev. Lett. **90**, 227902 (2003) [quant-ph/0211074]
J. I. Latorre, E. Rico, and G. Vidal, Ground state entanglement in quantum spin chains, Quant. Inf. and Comp. **4**, 048 (2004) [quant-ph/0304098].
- [64] U. Schollwoeck, The density-matrix renormalization group, Rev. Mod. Phys. **77**, 259 (2005) [cond-mat/0409292];
G. Vidal, Efficient simulation of one-dimensional quantum many-body systems, Phys. Rev. Lett. **93**, 040502 (2004) [quant-ph/0310089];
T. J. Osborne, The Dynamics of 1D Quantum Spin Systems Can Be Approximated Efficiently, Phys. Rev. Lett. **97**, 157202 (2006) [quant-ph/0508031];
J. Eisert, Computational Difficulty of Global Variations in the Density Matrix Renormalization Group, Phys. Rev. Lett. **97**, 260501 (2006) [quant-ph/0609051];

- N. Schuch, M. M. Wolf, F. Verstraete, and J. I. Cirac, Entropy scaling and simulability by Matrix Product States, *Phys. Rev. Lett.* **100**, 030504 (2008) [0705.0292];
A. Perales and G. Vidal, Entanglement growth and simulation efficiency in one-dimensional quantum lattice systems, 0711.3676;
N. Schuch, M. M. Wolf, K. G. H. Vollbrecht, and J. I. Cirac, On entropy growth and the hardness of simulating time evolution, *New J. Phys.* **10**, 033032 (2008) [0801.2078];
M. B. Hastings, Observations Outside the Light-Cone: Algorithms for Non-Equilibrium and Thermal States, 0801.2161.
- [65] M. Bauer and D. Bernard, 2D growth processes: SLE and Loewner chains *Phys. Rep.* **432** (2006) 115 [math-ph/0602049];
J. Cardy, SLE for theoretical physicists *Ann. Phys.* **318** (2005) 81 [cond-mat/0503313];
W. Kager and B. Nienhuis, A guide to stochastic Loewner evolution and its applications, *J. Stat. Phys.* **115**, 1149 (2004) [math-ph/0312251];
I.A. Gruzberg and L.P. Kadanoff, The Loewner equation: maps and shapes, *J. Stat. Phys.* **114**, 1183 (2004) [cond-mat/0309292].
- [66] O. Schramm, Scaling limits of loop-erased random walks and uniform spanning trees, *Israel J. Math.* **118**, 221, (2000) [math.PR/9904022].
- [67] A. Gamsa and J. Cardy, The scaling limit of two cluster boundaries in critical lattice models, *J. Stat. Mech.* (2005) P12009 [math-ph/0509004].
- [68] B. Doyon, V. Riva, and J. Cardy, Identification of the stress-energy tensor through conformal restriction in SLE and related processes, *Commun. Math. Phys.* **268** (2006) 687.
- [69] M. Bauer, D. Bernard, and K. Kytola, Multiple Schramm-Loewner Evolutions and Statistical Mechanics Martingales, *J. Stat. Phys.* **120**, 1125 (2005) [math-ph/0503024].
- [70] M. P. Mattis, Correlation functions in 2-dimensional critical theories, *Nucl. Phys. B* **285**, 671 (1987);
P. Arnold and M. P. Mattis, Operator products in 2-dimensional critical theories, *Nucl. Phys. B* **295**, 363 (1988).
- [71] P. Di Francesco, P. Mathieu, and D. Senechal, *Conformal Field Theory* (Springer-Verlag, New York, 1997).